

**A tidal stream energy resource assessment for Guernsey, UK,
with an investigation of the physical processes current
methodologies ignore.**

by

Joseph Leveson Wellerd

Thesis submitted to Plymouth University
in partial fulfilment of the requirements for the degree of
MSc Marine Renewable Energy

Plymouth University
Faculty of Science & Technology

in collaboration with
Guernsey Renewable Energy Team

September 2013

Disclaimer

The following document has been produced by a student at the University of Plymouth, working in partnership with the Renewable Energy Team, for their dissertation and so is an independent document. As such, while the study is endorsed by RET and was undertaken in conjunction with RET, there may be views expressed and conclusions drawn that are not shared by RET. There may also be some factual inaccuracies within the report, and whilst we appreciate them being brought to our attention, we are unable to alter them.

This copy of the thesis has been supplied on condition that anyone who consults it is understood to recognise that its copyright rests with the author and that no quotation from the thesis and no information derived from it may be published without the author's prior written consent.

Contents

1.0 Executive Summary	1
1.1 Abstract	1
1.2 Introduction.....	1
1.3 Aims and Objectives.....	3
1.3 Study justifications.....	4
2.0 Resource assessment methodologies.....	4
2.1 Overview	4
2.2 EMEC	4
2.3 EQUIMAR.....	4
2.4 Comparison of EMEC and EQUIMAR	5
3.0 Method	9
3.1 Overview	9
3.2 Data Acquisition	9
3.3 Data Handling.....	9
3.4 Data Analysis	9
3.4.1 Tidal Harmonic Analysis.....	9
3.4.2 Tidal Ellipse	10
3.4.3 Tidal current analysis	10
3.4.4 Velocity distribution curve and power exceedence graph	10
3.4.5 Power Calculation	11
4.0 Results	11
4.2 EMEC	13
4.1 EQUIMAR.....	19
5.0 Power output	21
6.0 Comparison of assessment results	22
7.0 Physical processes.....	23
7.1 Evidence of physical processes and discussion of impacts	23
8.0 Conclusions	28
9.0 Bibliography.....	29
10.0 Appendix.....	31

List of Figures:

Figure 1: Map of Guernsey with the islands of Sark and Herm and the Big Russel channel located. The data collection sites are also shown..... 2

Figure 2: Flow chart indicating the main stages of both resource assessment methods with common steps similar to each other in the centre coloured in orange and stages specific to individual methods. The side in red indicates the EMEC method, the yellow, EQUIMAR. Where the common steps have secondary, dashed boxes, these represent differences in the stage. 8

Figure 3: Depth averaged tidal velocity over data collection period for a) site 01 b) site 02 and c) site 03. Flood-ebb and spring neap cycles are labelled. 13

Figure 4: Maximum velocities over water column during data collection periods over flood and ebb tides at a) site 01, b) site 02 and c) site 03. 14

Figure 5: Velocity distribution curves for the three main depths at a) site 01 b) site 02 and c) site 03. The graphs show the occurrence likelihood of a velocity during the data collection period. 16

Figure 6: Tidal ranges calculated from tidal harmonic analysis a) site 01, b) site 02 and c) site 03. 17

Figure 7: Tidal ellipses of a) M2 and b) S2 tidal constituents over the 3 main water depths, tidal hodographs of c) neap and d) spring tides over the same water depths. 18

Figure 8: One tidal cycle taken from each data collection site of the spring and neap, compared with M2 and S2 tidal constituent over the same time period. (a) site 01 spring tide cycle, (b) site 01 neap tide cycle, (c) site 02 spring tide cycle, (d) site 02 neap tide cycle, (e) site 03 spring tide cycle, (f) site 03 neap tide cycle..... 19

Figure 9: Power exceedence graphs from 3 main water depths, a) site 01, b) site 02 and c) site 03..... 20

Figure 10: Tidal power, velocity cubed and velocity plotted over time for all 3 site from the top depth, 40.5 metres from ADCP. a) site 01, b) site 02 and c) site 03..... 21

Figure 11: Residual currents in the U and V flow directions taken from the mid depth a) Site 01 and b) Site 02. 24

Figure 12: Velocity depth profiles for 10 minute observation, front and side views. a) site 01, spring tide, on peak flood, b) side view of a), c)site 02, rotating tide, decimal time data 15.4230 2012., d) side view of c). Red arrow shows mean tide velocity, blue arrow shows M2 tidal constituent velocity, direction of North shown..... 25

Figure 13: Wave particle motions in deep water due to waves. (Holthuijsen, 2007) 26

Figure 14: Ekman layer at a flat seabed. Modified diagram from (Cushman-roisin & Beckers 2010). 26

List of tables:

Table 1: Showing the two resource assessments with each of their specific steps identified, where steps are share this is shown in orange, where only EMEC has the step, in red and where only EQUIMAR in yellow. The specifics of each step are described. 5

Table 2: Data collection periods 9

Table 3: Main tidal constituents 10

Table 4: Tidal constituents resolved from tidal harmonic analysis for site 01..... 12

Table 5: Tidal flow velocity data taken from long channel alignment with data converted into absolute values. Average velocity over 3 major depth groups and averaged over all 20 depth bins, with the maximum velocities observed. Showing all 3 data collection sites. Velocity in m/s^{-1} 16

Table 6: Power data for all 3 data collection sites. Power is calculated from long channel velocities. 22

Table 7: Flow direction within the BBL 27

Table 8: Bottom boundary layer depth 27

List of Equations:

Equation 1: EMEC Average Power Density 11

Equation 2: EMEC Power flux 11

Equation 3: EQUIMAR Available power/ Energy 11

Acknowledgments

Thanks are given to Guernsey renewable energy team who provided the ADCP data which made this research possible and their support through entire process. Also to Dr P Hosegood and Dr D Conley for their advice and counsel.

1.0 Executive Summary

1.1 Abstract

A tidal stream resource assessment is carried out using data obtained from a bed mounted acoustic Doppler current profiler (ADCP) carried out by Guernsey Renewable Energy Team, in the Big Russel channel and close to the island of Sark, Guernsey, UK. Two industry standard methods are used, the European marine energy centre (EMEC) assessment of tidal energy resource guideline and the Equitable testing and evaluation of Marine energy extraction devices in terms of performance, cost and environmental impact (EQUIMAR) deliverable D2.2 wave and tidal resource characterisation. These are summarised in tabular and flow chart format. The results of the two assessments are presented over 3 data collection sites with the overall power outputs calculated. Site 01 has the maximum power closely followed by site 02 and site 03 producing the least power available. Critique is made of the methods and results. The ADCP data is analysed and evidence of the effect of physical processes such as, wind and wave driven currents in the surface boundary layer (SBL), frictional effects of the sea bed in the bottom boundary layer (BBL) and turbulent flows are presented.

1.2 Introduction

The threat of climate change has seen governments all over the world shifting their countries energy production to cleaner sources. These sources include renewable energy. Using renewable energy reduces the dependence upon fossil fuel energy production and reduces carbon emissions into the atmosphere. (Baños et al. 2011) Marine current energy is in the form of kinetic energy. Water movements, which can be caused by tides, are concentrated through an area, due to constrained bathymetry. The tides which are governed by the gravitational effects of planetary movements give a predictable resource and the sites in which the energy can be exploited are numerous around the world. (AbuBakr S. Bahaj 2011) Guernsey lies in the English Channel, and is the second largest of the Channel Islands, close to the North coast of France. The Big Russel channel is the ideal area for the exploitation of tidal stream energy, shown in figure 1, due to its strong tidal current velocities, coupled with its close proximity to Guernsey's electricity grid.

This popularity in tidal stream energy has led the scientific community to develop methods for assessing the energy available at sites such as the Big Russel. There have been several methods for carrying out a tidal energy resource assessment. The European Marine Energy Centre, based in Orkney Scotland has published a set of guidelines (Marine Renewable Energy Guides) of which the Assessment of Tidal Energy Resource Guide is part. The document is aimed to provide guidance on how to

carry out a tidal energy resource assessment. Its purpose is to provide a standard methodology by which all tidal resource assessments can be carried out providing accuracy and consistency throughout the industry. It aims to calculate the potential power of extraction through measurement of the resource. (Legrand & EMEC 2009) The EQUIMAR protocols (2012) aimed to provide a set of standard boundaries in which the industry could carry out resource assessments. (EQUIMAR, 2012) An alternative method has been proposed in the US for assessing the potential impacts of extraction of energy associated with astronomical tides in the Beaufort River, USA. (Work et al, 2013) A framework which combined site and device suitability approaches was published in 2012 which aimed to assist identification of suitable locations for tidal stream energy using a modelling based approach. (Abundo et al. 2012) Another method, the TSE index, which is aimed to be used when selecting sites in depth-limited regions, provides users with a clear indication to whether the resource is good for extraction or poor. (Iglesias et al. 2012)

The two resource assessments this project will be focussing on are the EMEC and EQUIMAR methods.

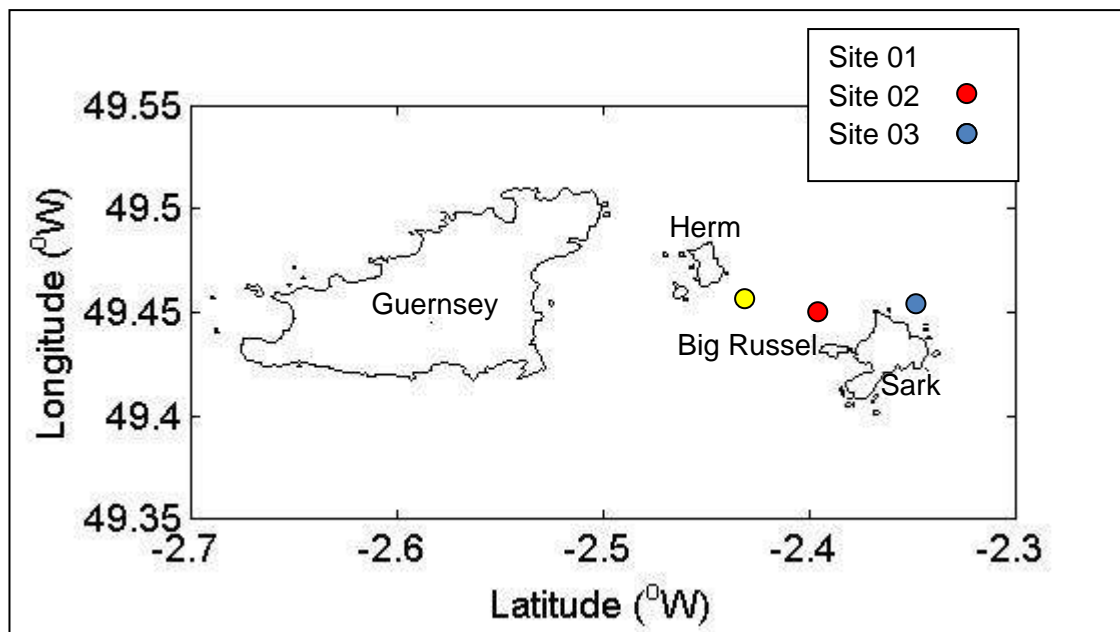


Figure 1: Map of Guernsey with the islands of Sark and Herm and the Big Russel channel located. The data collection sites are also shown.

There are numerous examples of tidal resource assessments carried out over the world's oceans. An assessment of the resource at Portland Bill, UK, where high tidal stream velocities are generated as currents flow around a headland, found that the tidal stream model which was used to predict features of the tidal cycle was useful and produced energy estimates of 730kW at peak output. (Blunden & A S Bahaj 2006) Considerably larger velocities were found in Passamaquoddy Cobscook Bays on the border of the United States and Canada. Current speeds in excess of 4 knots were

recorded. (Brooks 2006) In Alaska an assessment was carried out over 6 different areas. The cross-sectional area, average depth, the power density and the total kinetic power in the stream were measured. (Polagye, and Bedard 2006) Finally, research in the Alas Strait, Indonesia, assessing the tidal stream resource of the channel was carried out. The results included two scenarios giving practically exploitable annual energy yield at 330 GW h and 640 GW h. (Blunden et al. 2012)

One of the main issues with current tidal resource assessments is their lack of consideration of advanced physical processes occurring within tidal currents. Ignoring these can have serious implications on the accuracy of the overall power output calculated by the resource assessment methods. Assessments which simplify the physical processes in place in tidal flows considering only kinetic energy flux are shown to be overestimates of the actual available power. (Atwater & Lawrence 2011; Blunden & A. S. Bahaj 2007) The first step forward in turbulent flows was in 1883 where Reynolds published findings on the transition from laminar to turbulent flows.

Turbulence is created from the instability between shear flows. Where this occurs a three-dimensional rotational motion takes place. This motion causes small scale, large gradients of velocity, which leads to the creation of heat from frictional effects.

(Reynolds, 1883) This means that energy is dissipated throughout the water column, transferring from kinetic energy, key to tidal stream devices. (Osalusi et al. 2009) Work at EMEC's test site has shown the processes taking place within a tidal channel which can be resolved from ADCP measurements. The along-stream component of the Reynolds stress is shown to be related to tidal variations, ebb and flood, spring and neap processes. Reynolds stress with depth is observed to correspond with vertical structure of the mean shear and that the generation of turbulent kinetic energy is generally enhanced near the bed. (Osalusi et al. 2009) Turbulence can affect tidal ellipses, which are used heavily in tidal stream resource assessments.

1.3 Aims and Objectives

This study aims to compare and analyse two of the industry standard resource assessment methods popular within the marine renewable energy community at present. Comparisons of the methods and results of the two assessments will be presented. The data will also be analysed for the presence of physical processes which, if located, will be assessed for the impact on the results of the resource assessments.

- To resolve the differences and similarities between the two assessments.
- To gain a power output estimate from both resource assessments.
- To identify physical processes within the data
- To assess whether physical processes affect the results of the assessments.

1.4 Study justifications

Data is split into three main groups, top, middle and bed. The top group corresponds to data taken from the near sea surface environment, known as the surface boundary layer (SBL), at 40.5 metres from the ADCP, the middle group is at 10.5 metres distance from the ADCP, midway through the water column within the free stream environment and the bed group is 2.5 metres above the ADCP, in the bottom boundary layer (BBL). This allows for comparison of conditions throughout the water column.

The two resource assessments share several steps. These include tidal harmonic analysis and the calculation of tidal range. It has been deemed not necessary to repeat these stages within the assessments, will be noted included in the study. Stages which do not affect the results that this study is aiming to achieve will not be included within the study either. Both of the studied resource assessment methods address the influencing factor of meteorological and wave impacts in the surface waters, however neither attempt to resolve the effect. Consequently this study does not include the steps associated with these, but does investigate the effects.

2.0 Resource assessment methodologies

2.1 Overview

This section of the report will provide background information of the two resource assessment methods, with comparison of them. A table and flow chart is used to summarise the methods, highlighting the core and individual steps.

2.2 EMEC

The *Assessment of tidal energy resource guideline* (Legrand & EMEC 2009) was published in 2009 as part of the EMEC *Marine renewable energy guides* series. The main aims of the assessment are as stated: to measure and describe the resource (by deriving a velocity distribution for a site), to understand the potential for the power extraction of an array of TECS (by combining the velocity distribution with the power curve of the TECS), and to ensure that the tidal resource available is not over-extracted.

2.3 EQUIMAR

The EQUIMAR Wave and tidal resource characterisation deliverable (Venugopal et al. 2011) was published in January 2011 as part of a extensive study and consultation into marine renewable energy and the need of a structure for the industry to advance. The main aims of the resource assessment were: To describe established methods to characterise the marine environment for the purposes of resource assessment. To highlight the key oceanographic parameters relevant to ocean energy. To describe the principal applications of methods for the development of ocean energy projects.

2.4 Comparison of EMEC and EQUIMAR

The tidal stream resource assessments are assessed in Table 1 and the flow chart, Figure 2. The table is a description of the main steps involved in each of the assessments. Each steps details are outlined allowing for comparisons to be made between methods. The flow chart should be used to outline the major steps without specific details of each method. It allows the reader to see where the two methods differ and where steps are shared the method by which each assessment carries out that step.

Table 1: Showing the two resource assessments with each of their specific steps identified, where steps are share this is shown in orange, where only EMEC has the step, in red and where only EQUIMAR in yellow. The specifics of each step are described.

Stage of assessment	EMEC	EQUIMAR
Assess level of project (BOTH)	Determine level of resource assessment into set stages: Stage 1-Regional assessment-site screening, Stage 2a- Site assessment-pre feasibility, 2b-Site assessment- Full feasibility, 3- Site assessment- Design development.	Determine requirement for work: Energy resource level, Engineering design, Marine operations, Model verification. Determine level of resource: Early stage, Project development, Marine operations for the farm.
Determine if specific turbine design, and array size. (EMEC)	The general or specific requirements of the turbine if known are to be specified. The size of the array or farm is to be classified.	
Assessment of site conditions from previously available data(EMEC)	1. The bathymetric conditions are investigated with the level of project determining the requirement of survey. 2. The tidal range taken from two different gauges shall be taken at different resolutions: Annual, monthly and daily. 3.	

	Data describing the tidal currents should be presented.	
Constraints and available deployment area (EMEC)	The constraints of the project should be identified with the carrying out of an environmental scoping report above stage 2 and the physical constraints such as: MOD areas, pipelines and protected sites identified. The areas of bathymetry which do not allow the previously stated turbine size to be deployed should be eliminated from the study area.	
Selection of data collection method (BOTH)	Several options are selected for the collection of tidal data: Acoustic Doppler Current Profiler-vessel mounted for transect survey, static survey using ADCP at bed mounted location-deployment duration determined by stage of assessment.	Two options for tidal data collection are suggested: Acoustic Doppler profiler, Radar. Each is described in the literature highlighting its characteristics and issues with quality control.
Presentation of results (BOTH)	The results of the tidal harmonic analysis shall be displayed with the number of constituents stated and other required information as stated by the guidelines. Results of any other surveys to be included such as static survey with required details: Tidal velocity profile, depth averaged tidal profiles, vertical profile during max	Results of the data collection and tidal harmonic analysis should be displayed together contrasting the two primary constituents and the overall tidal flow with spring and neap tidal cycles indicated.

	flood and ebb and tidal range.	
Data analysis and presentation (BOTH)	<p>A histogram displaying the results from the tidal harmonic analysis should be displayed. This histogram will display the occurrence likelihood (% time) a current is at a set velocity. Each should be displayed for comparison and differences in shall be discussed. The maximum velocity from a month of the data, or as close to, will be compared to the average over the month. These values will be taken as depth averaged, at turbine hub height or average over the cross-sectional area of the turbine. The tidal range shall be displayed from the data. Tidal ellipses shall be made of the static field data of both spring and neap tides with. The directionality offset should be considered if the turbine design cannot rotate to align with the major axis of flow using the provided table within the EMEC method.</p>	<p>The current velocity should be displayed for the overall tide with the two primary constituents displayed also. This method is used to compare two different occasions such as: flood and ebb or spring and neap.</p>
Power calculations, analysis and presentation (BOTH)	<p>The average power density is calculated and over the cross-sectional area of turbine or channel from the measured/predicted velocity distribution.</p>	<p>Tidal power density is calculated over selected time periods for comparison between, as in current velocity analysis stage. From the tidal power density over time the skewness and variance can be</p>

		investigated. A histogram of power production exceedence is computed.
Turbulence analysis (BOTH)	A description of the different levels of turbulence observed should be made and consultation of recent research papers and reference to those.	Turbulence should be analysed with reference to recent research papers.

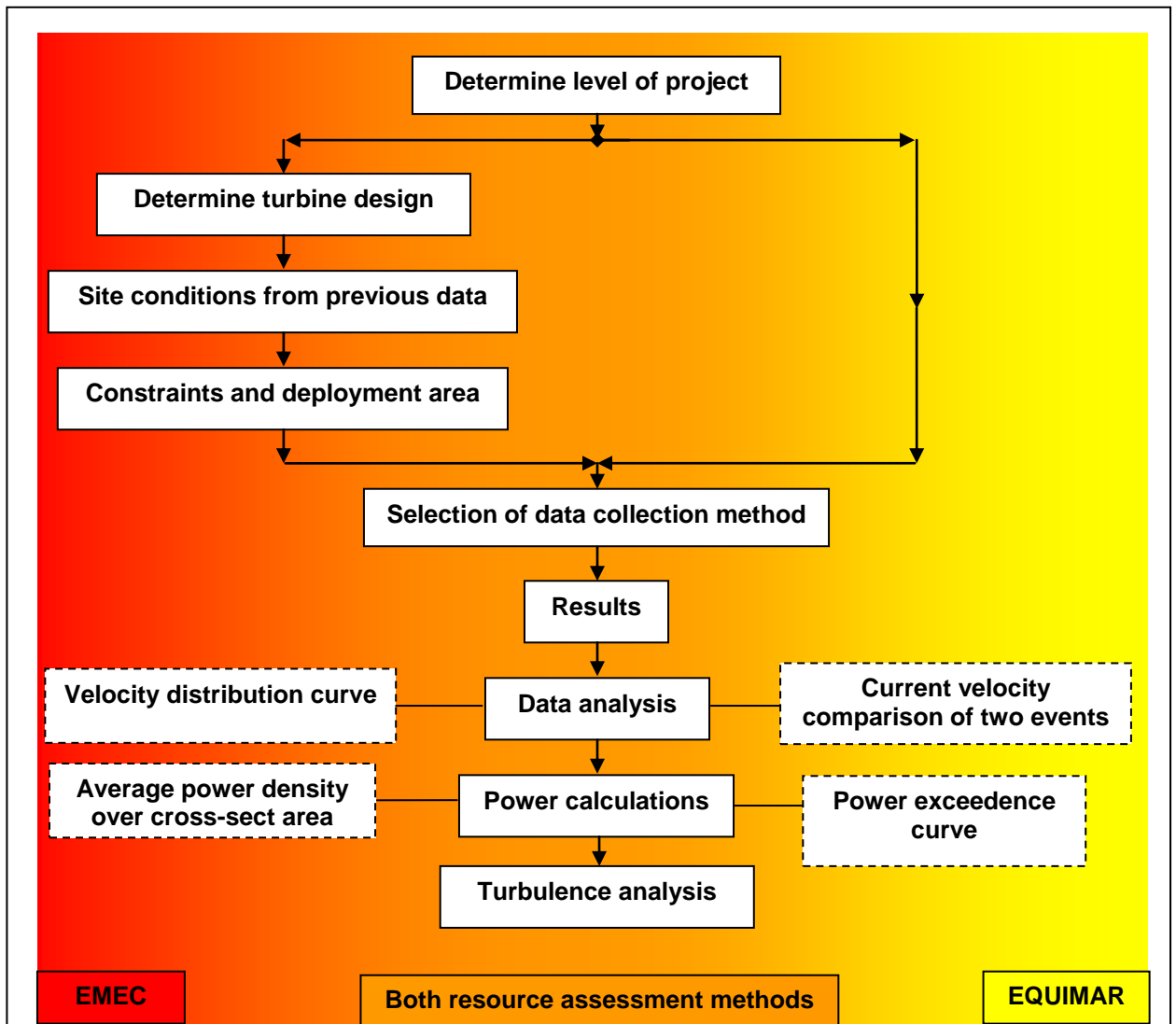


Figure 2: Flow chart indicating the main stages of both resource assessment methods with common steps similar to each other in the centre coloured in orange and stages specific to individual methods. The side in red indicates the EMEC method, the yellow, EQUIMAR. Where the common steps have secondary, dashed boxes, these represent differences in the stage.

3.0 Method

3.1 Overview

The resource assessments are carried out with data obtained from Guernsey Renewable Energy Team. Three static survey ADCP's being deployed around the area of the Big Russell channel, in locations identified in Figure 1.

3.2 Data Acquisition

Static surveys were working in 45 metres of water at 600kHz resolving at 2 metre vertical intervals. Data collection periods are shown in

Table 2.

Table 2: Data collection periods

Data Collection Site	Collection Period: Start - Finish (Date)
Site 1	14/11/2011 - 22/12/2011
Site 2	7/01/2012 - 7/02/2012
Site 3	20/2/2012 – 22/03/2012

3.3 Data Handling

The ADCP data was collected by GRET. Bad data was removed which was caused by the deployment and recovery of the ADCP device to the sea floor.

3.4 Data Analysis

3.0

3.3

3.4.1 Tidal Harmonic Analysis

Tidal harmonic analysis is used for predicting tidal heights, but can also be used for breaking down a measured tidal wave into individual driving components, known as constituents. Emery & Thomson (1997) describe it as a form of signal demodulation, breaking the wave down into predetermined frequencies where least-squares techniques are applied to solve the constituents. There are a maximum of 45 astronomical constituents. This study will use a mixture of these. Only those with a strong signal to noise ratio are used, for accuracy. Table 3 shows two the principal tidal constituents. A full list of the tidal constituents used is shown in appendix 4a. As the tidal signal is broken down into individual constituents, an unresolved signal, known as the residual will be left. This is made up of meteorological effects such as wave or wind driven current and other physical processes.

Table 3: Main tidal constituents

	Species	Period (hr)	Speed (°/hr)
M₂	Principal lunar semi-durnal	12.42	28.984
S₂	Principal solar semi-durnal	12	30

3.4.2 Tidal Ellipse

Tidal ellipses show the motion of the tide from a given point. They show the circular or elliptical nature of a tide, this is the eccentricity of the ellipse. This study will calculate the ellipse of the two major tidal constituents and the spring and neap tidal cycles. Tidal ellipses allow resolution of the major angle of flow at the centre of the ellipse known as the orientation or inclination. Plotting a tidal ellipse uses the tip of the changing vector of the tides velocity. This is plotted over a full cycle, for an individual constituent or spring or neap tidal cycle.

3.4.3 Tidal current analysis

The tidal data is primarily split over depth bins with each two metre depth a speed and direction. This is split into Northerly (U) and Easterly (V) components.

The U and V tidal components are then split into long channel flow and cross channel flow. This is calculated by aligning the flow with the angle which the semi-major axis of the M2 tidal component is at. The M2 tidal constituent is used as it is the dominant constituent, the lesser constituents such as the S2 and N2 have semi-major axis very close to that of the M2.

The maximum flood and ebb tidal profiles are calculated by selecting the maximum tidal velocities over the water depth during the peak flood and ebb cycles, during the spring tidal cycle.

The tidal range is calculated using the pressure output from the ADCP.

3.4.4 Velocity distribution curve and power exceedence graph

The tidal velocity curve displayed within the EMEC assessment and the power exceedence curve used in the EQUIMAR method are calculated with similar methods. Each uses a histogram, EMEC calculates the percentage over time at which the flow is at a given velocity. EQUIMAR uses the amount of time which the tidal flow can provide power over a value, and the cumulative sum of the percentages.

3.4.5 Power Calculation

Both the resource assessments overall goal is to compute a power output from the given data. Both methods use similar methods for resolving the power. EMEC splits it into two different sections, first the calculation of the average power density as shown in:

Equation 1: EMEC Average Power Density

$$- - \quad (kW / m^2)$$

Where j is the index of the 10 min increments, V_j^3 is the velocity cubed recorded every 10 min, N is the total number of time intervals (= total period of simulation divided by 10 min) and ρ = water density (1025 kgm³).

This calculates power at a given point. To calculate over an area, shown below as $A_{channel}$, but can be used over any area, such as the cross-sectional area of a turbine.

Equation 2: EMEC Power flux

The EQUIMAR method uses a much more concise method, but still using the same basic method.

Equation 3: EQUIMAR Available power/ Energy

4.0 Results

4.1 Data processing

Tidal harmonic analysis was carried out on each data collection site, the constituents with strong signal to noise ratio used by the analysis are shown Table 4, with sites 02 and 03 in appendix 4. The M2 constituent is by far the largest contributing force. This is apparent from the semi major value. This extends over all of the sites. The second largest contributor is the S2 constituent. It should be noted that both these constituents have an inclination, angle at which the semi major is orientated, within 2 degrees of each other for defining the long channel axis. The other sites show a similar trend of close orientation.

The U and V components of the tidal stream at site 01 are shown in appendix 1. These are used, as described within the method, as a stepping point for calculation of the long and cross channel velocities. They show the initial step of splitting the data from a

Table 4: Tidal constituents resolved from tidal harmonic analysis for site 01.

Tide	Freq	Major	Minor	Inc	Pha	Snr
MSF	0.0028219	0.114	0.032	58.06	166.26	3.4
ALP1	0.0343966	0.033	-0.001	112.69	29.79	2
Q1	0.0372185	0.038	0.011	100.45	178.43	2.6
O1	0.0387307	0.035	0.005	55.96	45.34	2.1
EPS2	0.0761773	0.035	-0.022	12.96	331.85	2.2
MU2	0.0776895	0.045	-0.030	142.86	84.08	3.5
N2	0.0789992	0.306	0.021	57.70	250.69	88
M2	0.0805114	1.620	0.062	60.45	125.88	1.8e+003
L2	0.0820236	0.141	0.007	56.12	203.18	18
S2	0.0833333	0.368	-0.006	57.87	285.15	1.2e+002
MN4	0.1595106	0.064	-0.010	37.45	270.93	6.5
M4	0.1610228	0.152	-0.017	27.84	166.07	50
MS4	0.1638447	0.070	0.011	11.71	315.44	10
2MN6	0.2400221	0.037	-0.009	59.14	53.69	4.6
M6	0.2415342	0.071	-0.021	52.76	295.47	18
2MS6	0.2443561	0.042	-0.008	51.73	69.70	6.7
M8	0.3220456	0.040	0.003	14.36	324.2	12

single speed with a direction, into a velocity. The data shown in appendix 2 shows that at site 01 the larger proportion of the tide is aligned with the Northwards component, as the velocity range is greater, it also shows how this changes with depth.

The long and cross channel velocities are now calculated. These are obtained by use of the semi major axes from the tidal harmonic analysis. As described earlier the M2 and S2 tidal constituents are used to obtain this. The long and cross channel aligned flow is shown in appendix 2. The long channel data is considerably higher than the cross channel component. This also shows differences in velocity over the vertical within the water column. It is observed that the top and middle of the water column have higher velocities than those at the bed, which are considerably lower.

4.2 EMEC

The depth averaged tidal profiles for each of the sites are shown in Figure 3. The flood and ebb tides are labelled, two cycles per day this classifies it as semi-diurnal. The spring and neap tidal cycles are also labelled, the spring tides where the velocities are highest and neaps where they are least. As the data here is depth averaged it means the velocities are averaged over the entire depth. This allows comparisons to be made spatially over different sites and temporally, but not in the vertical axis.

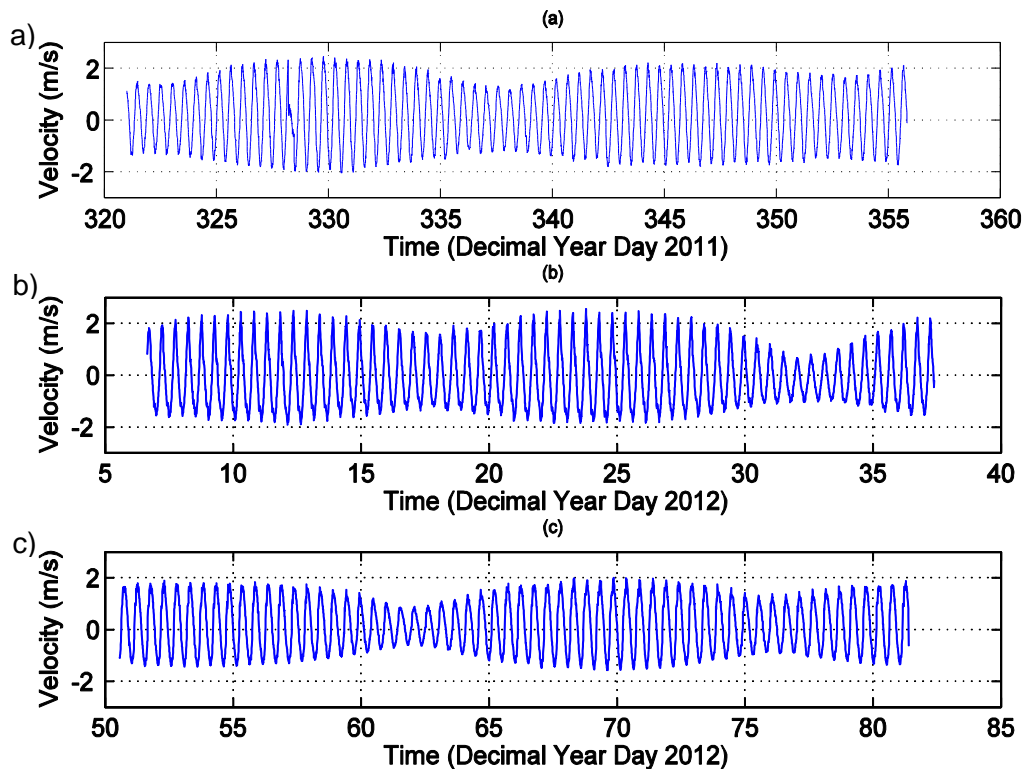


Figure 3: Depth averaged tidal velocity over data collection period for a) site 01 b) site 02 and c) site 03. Flood-ebb and spring neap cycles are labelled.

The maximum velocities observed over the tidal cycles are displayed in Figure 4. These show the maximum velocities at each depth. The velocities are split into flood and ebb over all sites. This indicates a trend of the flood and ebb tide in the Big Russel area. All three sites show the flood tide having higher maximum velocities than those on the ebb. The differences in the vertical should also be noted. As discussed earlier, the velocities in the middle of the water column are higher than those at the bed. The general trend is the closer to the sea bed, the lower the velocities. This is also true at the water's surface in several cases. Site 01 on the ebb reduces as it nears the water's surface and on the flood and ebb of site 02.

Comparisons across the 3 different sites can be made from

Table 5. It illustrates the differences between the average values and the maximum values. The average maximum value of site 02 is higher than that of site 01, however site 01 has a higher average tidal velocity. It also shows the lower velocities observed at site 03 compared to the other sites. The lower flow velocities at the bed are clear here also. The mid and top velocities are approximately 0.5m/s lower at sites 01 and 02 and less at site 03.

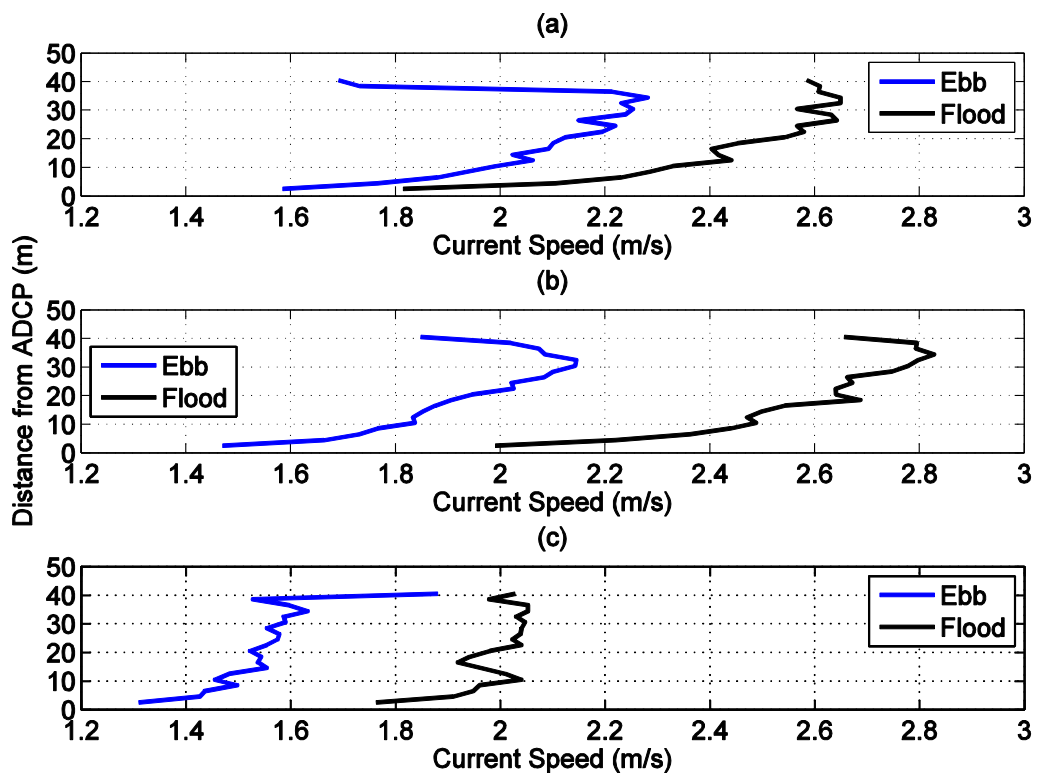


Figure 4: Maximum velocities over water column during data collection periods over flood and ebb tides at a) site 01, b) site 02 and c) site 03.

The velocity distribution curves shown in Figure 5 present data from all three sites at the top, middle and bed depths.. The graphs show the percentage of the overall time that the water was moving at a set velocity. It can also be described as if you were to randomly pick a moment during the data collection period how likely it would be for the water to be moving at that set velocity. For example at site 01 at bed depth the tidal flow was moving at 1m/s for approximately 9% of the time. The data used for the velocity distribution curves is obtained from the

tidal harmonic analysis, which are predicted values, this explains the differences in maximum values to that of the observed data which are real life values, such as those in

Table 5. At site 01 the top and mid depths within the water column are moving at similar in velocities as the lines follow each other closely. The water movement at the bed has much lower velocities as it shows a higher percentage of time spent at lower velocities, from 0 to approximately 1 m/s, it reaches 0% of time at approximately 1.6m/s. Site 02 shows a similar pattern, however, the top and mid depths peak above 2.5 m/s. The data from site 03 shows the same pattern, but at lower velocities.

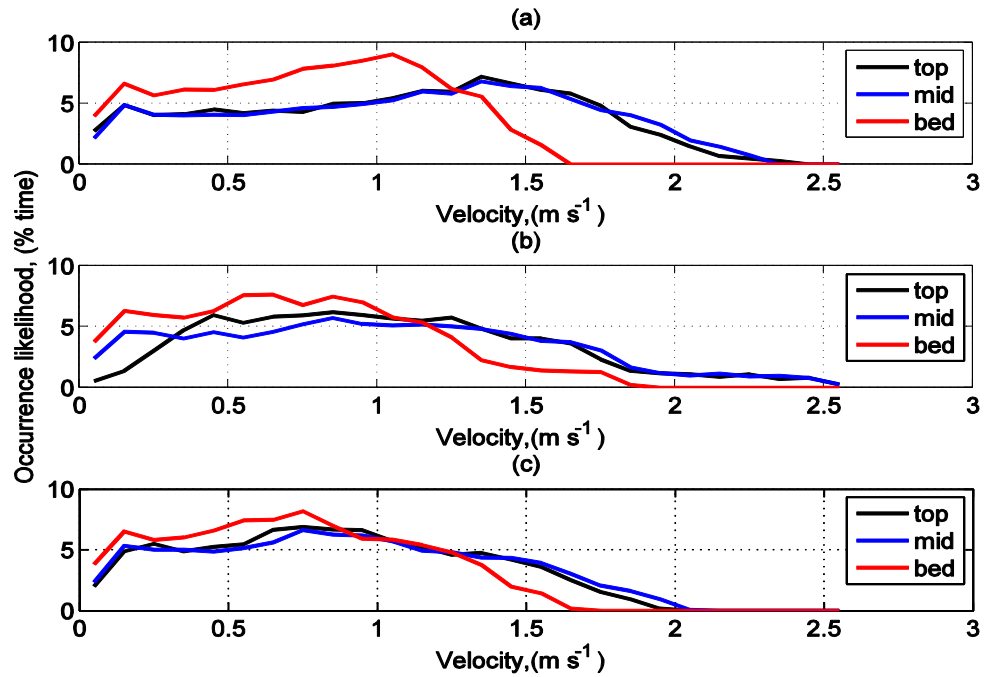


Figure 5: Velocity distribution curves for the three main depths at a) site 01 b) site 02 and c) site 03. The graphs show the occurrence likelihood of a velocity during the data collection period.

Table 5: Tidal flow velocity data taken from long channel alignment with data converted into absolute values. Average velocity over 3 major depth groups and averaged over all 20 depth bins, with the maximum velocities observed. Showing all 3 data collection sites. Velocity in m/s^{-1} .

Site 01			Site 02		
Depth	Average velocity over time	Max velocity over time	Depth	Average velocity over time	Max velocity over time
Top	1.0738	2.6594	Top	0.9997	2.6520
Mid	1.1102	2.6046	Mid	1.0388	2.7085
Bed	0.7792	1.9844	Bed	0.7503	2.1458
Average over all depths	1.0638	2.4542	Average over all depths	0.9910	2.5780
Site 03					
Depth	Average velocity over time	Max velocity over time			
Top	0.8895	2.1364			
Mid	0.9921	2.1186			
Bed	0.7445	1.8825			
Average over all depths	0.8945	2.0038			

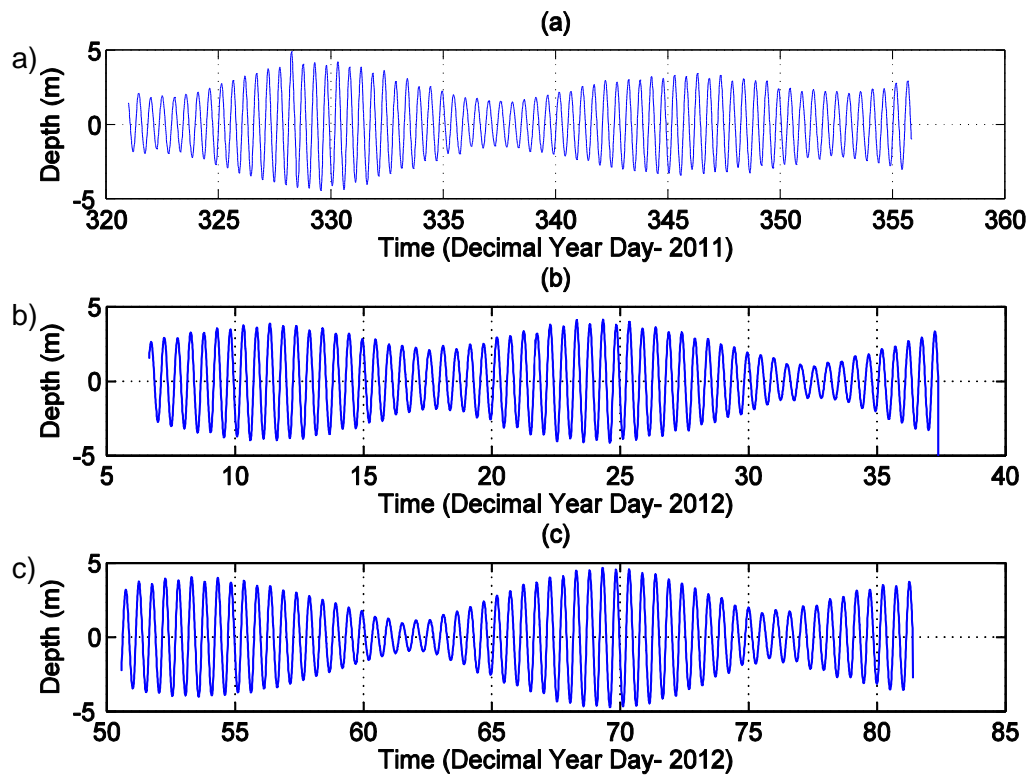


Figure 6: Tidal ranges calculated from tidal harmonic analysis a) site 01, b) site 02 and c) site 03.

Tidal ellipses are required by the EMEC method to be calculated, however the spring and neap “ellipses” are technically known as hodographs, as they do not centre on 0. Figure 7 shows the ellipses at site 01. The M2 and S2 components are displayed. The M2 ellipses show a pronounced elliptical shape with high eccentricity, with little change over depth. When compared to the S2 ellipses the M2 is approximately 1m/s greater in a single direction from the centre point, illustrating the dominance of the M2 tide. This is also true for sites 02 and 03 shown in appendix 3. This would suggest that the waters of Guernsey are heavily dominated by the M2 tidal constituent. The angle of the ellipses is important when considering the use of a turbine which cannot rotate its axis, such as the OpenHydro device (Previsic et al. 2005), which is mounted on the bed. The alignment of the device to optimise collection would be based on results from these ellipses. The spring and neap tidal cycle hodographs are also shown. These were obtained from the real life data taken from the ADCP. The spring tidal hodographs are larger than those on the neap. The main difference between the two is the shape of the hodographs. The spring tides vary in direction more than the neap. In appendix 3 the sites 02 and 03 hodographs also show the variable direction of the tide. All of the spring and neap tidal hodographs cross over as they change from flood, the positive

flow, to ebb, negative flow, and vice versa. When comparing the M2 and S2 tidal constituent ellipses to the spring and neap hodographs it is clear that the constituents rotate around a central point, 0, however this is not the case for the spring and neap. There is an offset of the centre observed, this is seen greatest over the spring tides. The neap tides have a central point closer to 0. The hodographs show a trend of the central point placed towards the South East of 0. The most extreme case of this central point offset is at site 02 from the top hodograph, this is also observed at the neap hodograph, but in the opposite direction. It should be noted that the spring and neap hodographs were collected from real time data, so are susceptible to meteorological and wave forced currents and localized bathymetric forcing upon the flow, whereas the constituents from tidal harmonic analysis are purely predicted mathematically so are not subject to this. The shape of the hodographs over the spring and neap cycles over the vertical can also be compared. For the most part they show a very similar pattern, the mid is the largest, the top less and the bed having the lowest velocity difference. At site 02, neap cycle, the top hodograph has a very different shape to the other depths. This suggests that it is influenced by wind or wave currents, which only penetrate the upper water depths, where the top hodograph is representing flow.

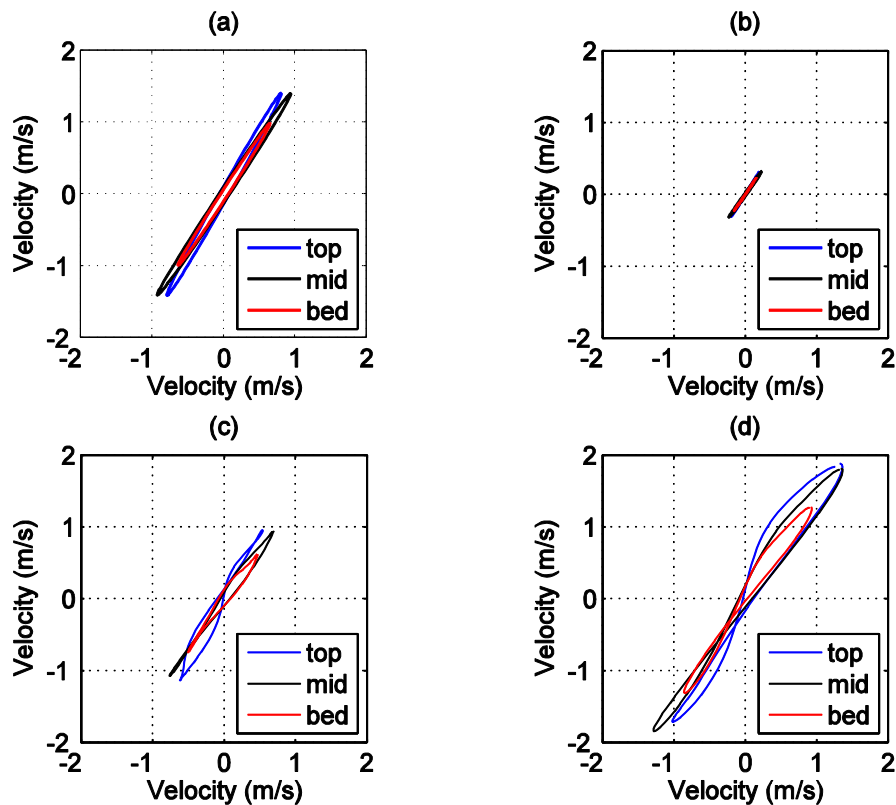


Figure 7: Tidal ellipses of a) M2 and b) S2 tidal constituents over the 3 main water depths, tidal hodographs of c) neap and d) spring tides over the same water depths.

4.1 EQUIMAR

The results of the EQUIMAR resource assessment are presented in this section. *Figure 8* shows tidal cycles obtained from each site at the mid depth, 10.5 metres above the ADCP, a flood and ebb tide are observed. This figure shows the difference in velocity characteristics between spring and neap tides. The spring tides have larger velocities compared to the neap. The relative influences of the M2 and S2 tidal constituents upon the overall tidal cycle are noticeable. Part (a) has vertical lines indicating the position of the flood and ebb of the long channel velocity, with the distance between indicated as the wavelength. The M2 and S2 constituents are labelled also. The relative positions of peaks and troughs of the M2 and S2 influence the characteristics of the overall tidal movement. The impact of the M2 is best shown in part (a), the M2 and tidal flow are close to being in phase, the long channel velocity is at its greatest here, being

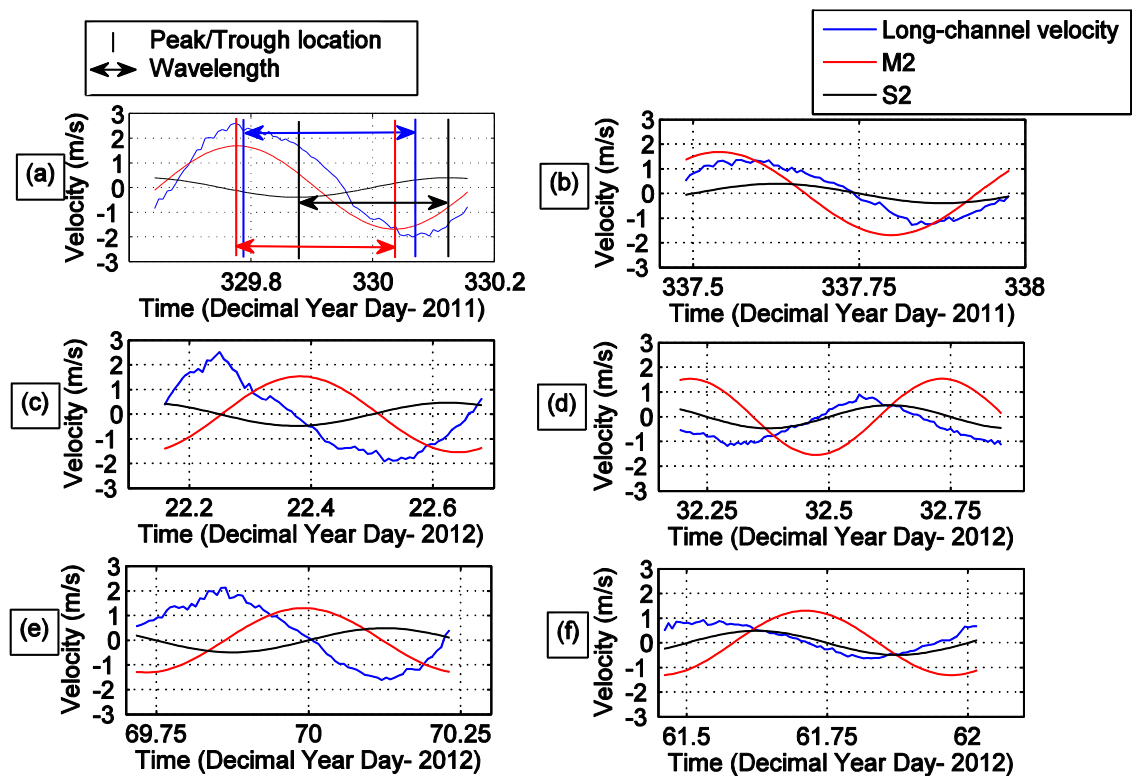


Figure 8: One tidal cycle taken from each data collection site of the spring and neap, compared with M2 and S2 tidal constituent over the same time period. (a) site 01 spring tide cycle, (b) site 01 neap tide cycle, (c) site 02 spring tide cycle, (d) site 02 neap tide cycle, (e) site 03 spring tide cycle, (f) site 03 neap tide cycle.

influenced by the M2. Over the neap tides shown in parts (b), (d) and (f) the long channel tide is closely matched to the shape of S2 tidal component and out of phase with the M2.

Although the calculations of power will be presented in the following section, graphs for the EQUIMAR method which use power are analysed here. The first shows the power

density, velocity cubed (stream power), and the velocity in the long channel axis over a tidal cycle containing a flood and ebb tide *Figure 9*. The two peaks represent the flood and ebb, as labelled. The flood tide dominance is noticeable, as it generates a significantly greater power. The relationship between power and velocity is also shown. The power density and the velocity cubed are directly related, whereas the velocity and powers is not as clear. This is because the power is directly proportional to the velocity cubed, as shown in Equation 1 and Equation 3. The difference in power generation is revealed across the three sites. It is clear that during the spring tide, when this data is taken, site 01 generates a larger amount than site 02 and for a longer period, and site 03 generates a smaller amount of power for a shorter amount of time.

The power production exceedence is the percentage of time that a tidal flow has

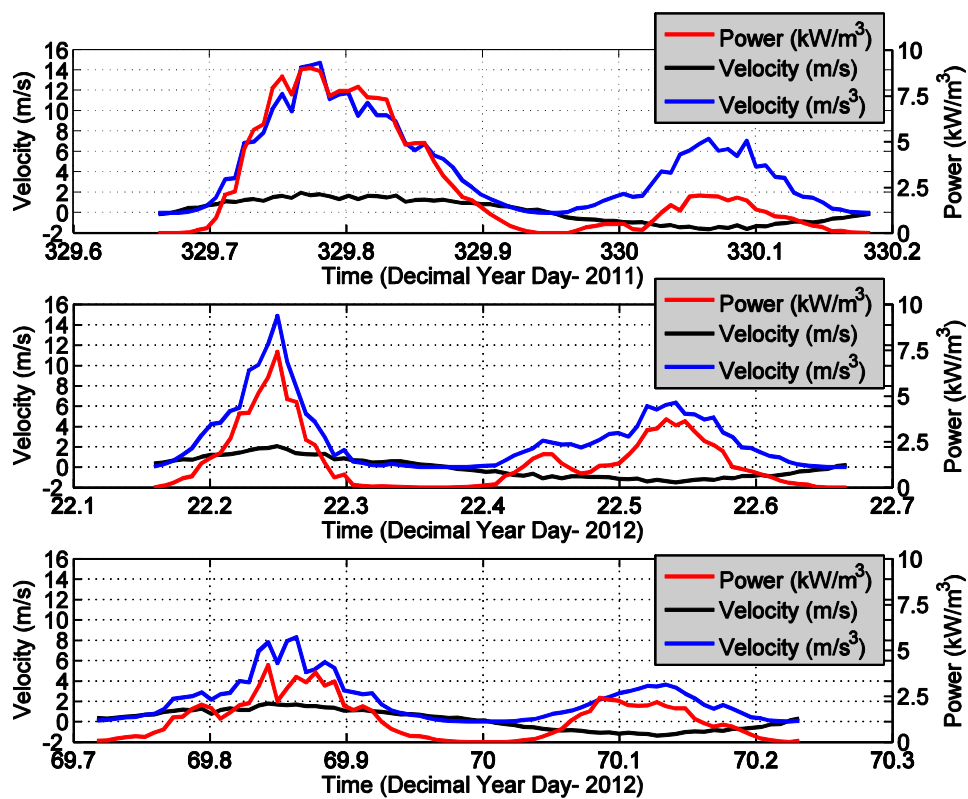


Figure 9: Tidal power, velocity cubed and velocity plotted over time for all 3 site from the top depth, 40.5 metres from ADCP. a) site 01, b) site 02 and c) site 03.

stream power available, over a set value. *Figure 10* presents the power exceedence graphs at site 01. The top and mid depths are very close and the bed reduces at a lower stream power. This is repeated over the other sites, except, moving through numerically through the sites, the difference between the top and mid depths and the bed values reduce.

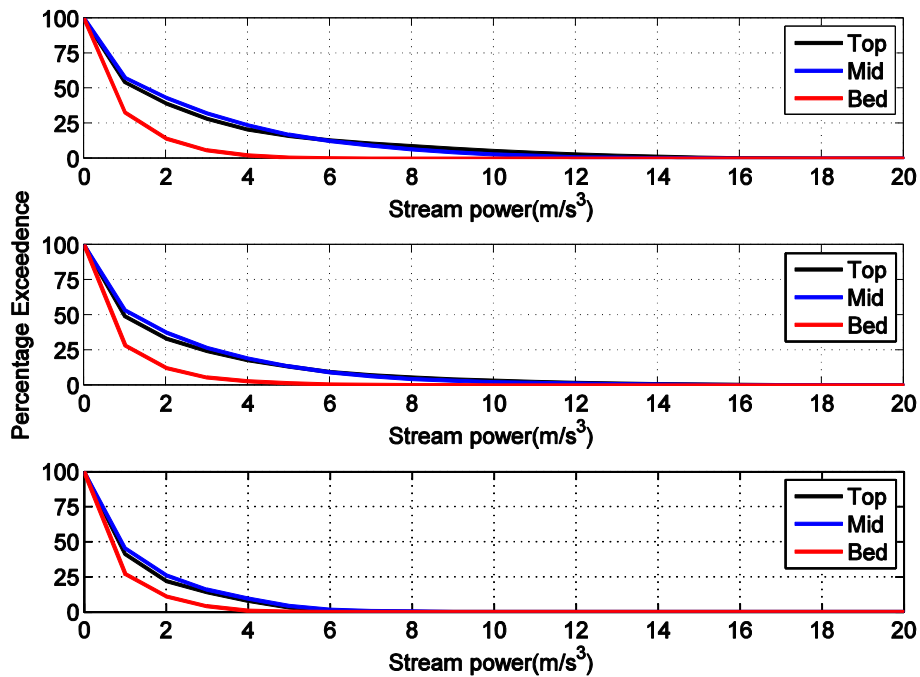


Figure 10: Power exceedence graphs from 3 main water depths, a) site 01, b) site 02 and c) site 03.

5.0 Power output

The two resource assessment methods use the same overall method to calculate the power available from the tidal stream, results are shown in Table 6. Each method calculates the power available over different spatial scales, at a single point, kW/m^3 and over the cross-sectional area such as the channel width or a tidal turbine. The OpenHydro device is used to represent power levels over a typical device (Previsic et al. 2005). It has a cross-sectional area of 318m^2 . The average power available, maximum power and total power over the data collection period is shown. Site 01 has the highest levels total power available, with site 02 slightly less and site 03 the least. An interesting comparison can be observed between the max power levels at site 01 and 02. Site 02 has higher maximum power levels, whereas site 01 has a higher average. This demonstrates that the peak power is not the most important factor for a tidal stream power location and that the entire tidal cycle should be taken into account to gain maximum overall power. The difference in power available over the vertical plane is shown to be significant, the mid depth is slightly greater than the top, furthermore the bed levels are significantly less, at sites 01 and 02 the amount at the bed is greater than half that of the upper depths. As the power available reduces at site 03, the difference between bed and upper depths reduces, but is still significant. The power available calculated from each of the sites shows that site 01 would be the optimum for tidal stream power production, as it has the largest total power available

over the timescale measured. Site 02 would be the second choice and 03 the third best.

Table 6: Power data for all 3 collection sites. Power is calculated from long channel velocities.

Site 01						
Depth	Total power available device (kW) over data collection	Total power available (kW/m³) over data collection	Max power available device (kW)	Max power available (kW/m³)	Average power available (kW/m³)	Average power available from device (kW/m³)
Top	2065300	6494.6	3065.2	9.639	1.294	411.576
Mid	2069200	6507	2879.5	9.055	1.297	412.36
Bed	726930	2285.9	1273.4	4.005	0.456	144.864
Average over all depths	1823700	5734.8	2409	7.575	1.143	363.422
Site 02						
Depth	Total power available device (kW) over data collection	Total power available (kW/m³) over data collection	Max power available device (kW)	Max power available (kW/m³)	Average power available (kW/m³)	Average power available from device (kW/m³)
Top	1523300	4790.2	3039.7	9.559	1.0818	344.008
Mid	1575100	4953.2	3238.1	10.183	1.1186	355.718
Bed	606960	1908.7	1610.2	5.064	0.4310	137.074
Average over all depths	1386000	4358.4	2792.4	8.781	0.9843	313.005
Site 03						
Depth	Total power available device (kW) over data collection	Total power available (kW/m³) over data collection	Max power available device (kW)	Max power available (kW/m³)	Average power available (kW/m³)	Average power available from device (kW)
Top	917470	2885.1	1589.3	4.998	0.65	206.638
Mid	1020700	3209.8	1549.9	4.874	0.723	229.893
Bed	554260	1742.9	986.5	3.102	0.393	124.833
Average over all depths	922280	2900.3	1311.2	4.123	0.653	207.721

6.0 Comparison of assessment results

The two resource assessment methods share a core relationship carrying out the same main steps, as shown in Figure 2, however the method for carrying out these steps vary. The first comparison in methods is between the use of power available and

velocity. The goal of these graphs is to calculate the amount of time that the tidal flow will be at a set level. The EMEC method uses a velocity distribution curve, Figure 5 to analyse the percentage of time that a site will be at a specific velocity. The EQUIMAR method uses a similar process of a histogram, Figure 10, but with the percentage of time the stream power will exceed a set level. Equation 1 and Equation 3 show that power uses the velocity cubed, not velocity. A small difference in velocity can be a very large difference in velocity cubed. At site 01 the peak velocity between the flood and ebb at the mid depth, 20 metres, is approximately 0.4 m/s, Figure 9. In contrast to this the difference in velocity cubed is approximately 7m/s^3 and 14kW/m^3 of available power. This would suggest that as a tidal stream site is chosen on its available power output the EQUIMAR method of analysing power would be the ideal route.

The second comparison in methods is the route which calculates the relative influence of the tidal constituents over the tidal cycles. EMEC uses the calculation of tidal ellipses from the results of the tidal harmonic analysis and EQUIMAR uses the peak and trough positions of the constituents relative to the measured tidal cycle. The EMEC method is quantifiable; it uses real values such as the semi-major axis, for gauging the size relative to the other constituents and the inclination, the angle at which the tidal ellipse is aligned. Although the EQUIMAR method carries out tidal harmonic analysis, it does not use it for this. The method which compares the position of individual peaks and troughs and the overall shape of the tidal constituents and tidal flow is subjective, where two individual resource assessments carried out by different groups may interpret the data differently according to difference in opinion.

7.0 Physical processes

6.0

7.0

7.1 Evidence of physical processes and discussion of impacts

Although the two resource assessment methods acknowledge the presence of physical processes, neither allow for the effect on the results. Within the EMEC method the depth averaged velocity is often used, assuming the flow is uniform over depth, laminar flow. However, from the results of the two resource assessments it is clear that the flow is not uniform over depth and there are numerous variations of velocity. The tidal harmonic analysis splits the flow into components controlled by tidal constituents, but it does not account for the entire flow.

The residual currents, shown in Figure 11, are the parts of the tidal flow not accounted for by astronomical forcing; they are shown to be up to and slightly greater than 0.5 m/s

of the overall tidal flow. It can be explained by the un-quantified physical processes acting in the water column.

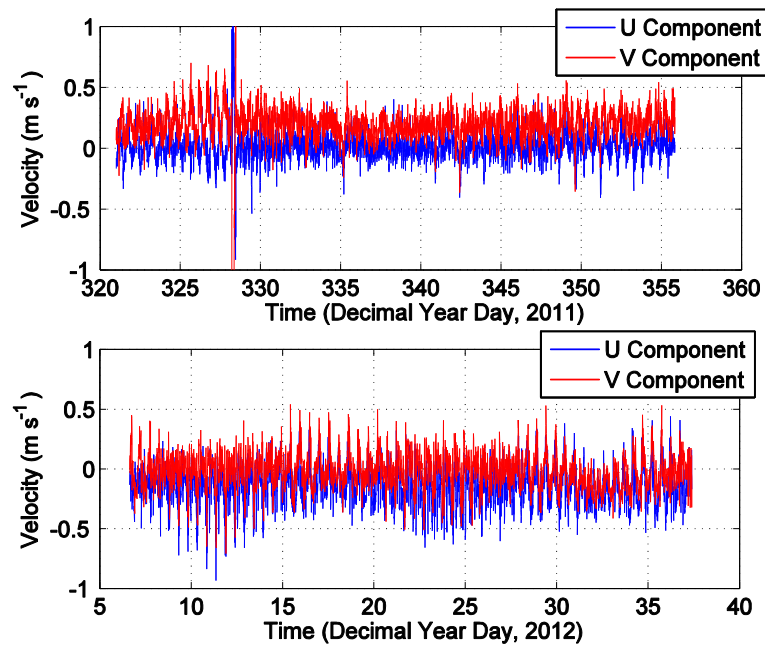


Figure 11: Residual currents in the U and V flow directions taken from the mid depth a) Site 01 and b) Site 02.

Wind blowing over the surface of water creates collisions between the two bodies, this causes the water to move, causing a water current. Once the current is generated, it exerts a frictional force on the water below it, causing movement in that too, resulting in movement to be transferred down through the water column. The greatest movement is at the surface with the speed of the water current diminishing with depth. With the increase in depth the direction of the current also changes, this is due to the Coriolis deflection. In the Northern hemisphere this causes current to turn to the right of the current above at approximately 45 degrees in theory, in real conditions it is less. The result is a spiralling flow pattern over depth, known as the Ekman spiral. For this process to set up it requires a consistent wind blowing over water for an extended period, however, for a surface wind driven current to be setup takes less time. (Pinet, 2006) Figure 12 displays tidal velocity profiles, the tidal direction and speed over the collected depths taken during springs on a flood tide. Both sites show change in direction with depth. Site 01 shows less change in direction in the top half of the water column, whereas at site 02, between 40.5 metres from the ADCP to 26.5 metres the direction of flow rotates towards the East with depth. Between 26.5 and 14.5 metres the flow then rotates back to the North and after 14.5 metres to the East. Figure 12 also shows the reduced velocities in the depths close to the sea bed. The magnitude of wind driven currents is discussed by Zhigang & Bowen (1992) where the currents are modelled.

Another effect of interaction between the air flow of the atmosphere and the water's surface is the development of waves. As the wind moves over the water's surface the

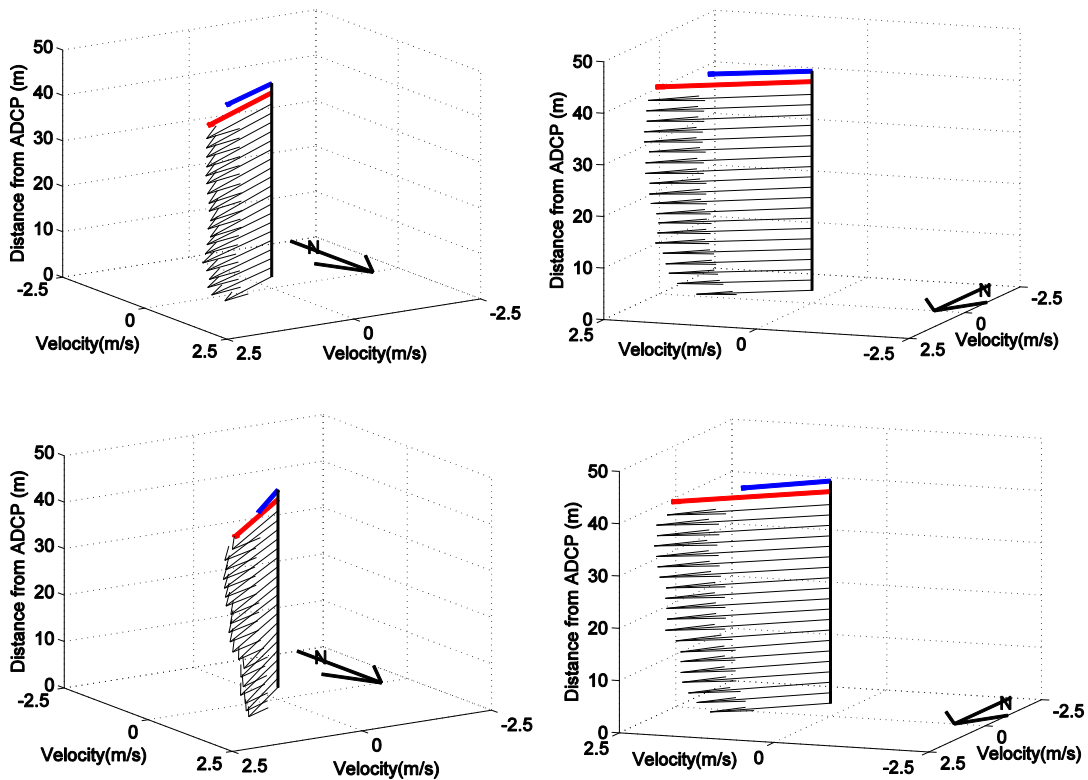


Figure 12: Velocity depth profiles for 10 minute observation, front and side views. a) site 01, spring tide, on peak flood, b) side view of a), c) site 02, rotating tide, decimal time data 15.4230 2012., d) side view of c). Red arrow shows mean tide velocity, blue arrow shows M2 tidal constituent velocity, direction of North shown.

friction between the two causes the water to be formed into waves. At low wind speeds capillary waves are formed, which quickly die out, however with an increase in wind speed these waves are transformed and grow into gravity waves, chop or swell. Underneath the surface, the waves cause movement of the water particles into a series of orbital motions which are illustrated in Figure 13. The motions are also assessed in Ehrnström & Villari (2008). The size of these flows are assessed by (Storlazzi et al. 2004), the conditions in which the measurements are made are over a reef and in shallow water, however the magnitude of the flow is relevant to be used as an estimate for comparison. The study presents wave orbital motions at 0.14 m/s at 0.2 metres above the bed being carried out in approximately 10 metres water depths. The waves were measured at between 0.2 and 0.4 metres. Furthermore, a study by Van Rijn et. al. (1993), which includes wave particle water motion, presents that the wave current can be increased or reduced depending on whether following or opposing the overall current. It states that wave currents in 0.5 metres water depth, with waves heights of 0.15 metres and a period of 2.5 seconds are at 0.025 m/s following the current and 0.03 m/s opposing the current. This study investigates small waves whereas the waves

in the Big Russel are larger, which would increase the wave driven currents. Modelled data of the wave climate around Guernsey is made by Magar et al. (2013) between Jan 2009 and Jan 2010, wave heights vary between approximately 0.5 and 3 metres with peaks of between 4 and 6 metres during extreme periods during the winter. This study was carried out during the winter months when wave heights were largest during Magar's study. Zhigang & Bowen (1992) also discuss the velocities associated with wave driven currents.

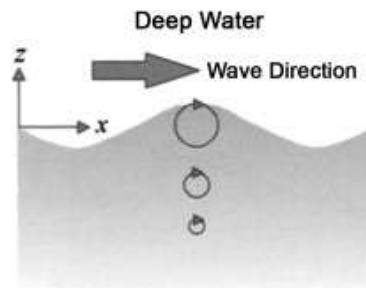


Figure 13: Wave particle motions in deep water due to waves. (Holthuijsen, 2007)

At the bottom of the water column, close to the seabed, is the bottom boundary layer (BBL). The size of which is determined by the interaction between the seabed and the water flowing over it. This study defines the BBL extending from a height at which the flow velocity is less than 90% of the mean flow. Table 8 shows the results of this definition, at sites 01 and 02 the flow drops below 90% at 4.5 metres depth.

As observed from the results of the resource assessments and the data shown in Figure 12 illustrates the reduction in velocities seen at the depths close to the sea bed. This reduction of current speed is due to the turbulent drag inflicted on the water movement from the sea bed, this is a frictional stress. As seen at the surface, an Ekman flow direction change is created, known as Ekman veering. The changes in direction of the flow seen in Figure 12 over the vectors closest to the seabed are a result of this. These areas are normally characterised by high levels of turbulence. (Simpson & Sharples, 2012)

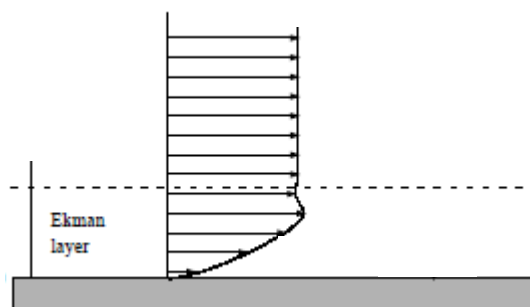


Figure 14: Ekman layer at a flat seabed. Modified diagram from (Cushman-roisin & Beckers 2010).

Figure 14 shows a diagram of the flow retardation which occurs due to frictional influence of the sea bed on the water movement. It shows a “perfect” example, where the flow is reduced to 0 at the bed and above the Ekman layer the water flow is uniform. Evidence of Ekman veering has been investigated by Kundu (1976) where values of between 5-15 degrees were observed off the coast of Oregon, and by Saylor & Miller (1988) observing veering averaging at 11 degrees in Lake Michigan. This study has seen Ekman veering of lower values, Table 7. Site 01 shows a maximum difference between the 2.5 and 4.5 metres depths of approximately 3° whereas the mean BBL direction compared to the mean overall flow direction is 1.35°. This trend is not repeated at site 02, where the difference between 2.5 and 4.5 metres is less at 0.34°, whereas the mean flows difference is 2.25° greater than that at site 01. From the bed the water above the bed alters to the left, in a bottom derived Ekman spiral. The results also show that at site 01 the 4.5 m water veers to the left of the 2.4 m direction, the correct direction for Ekman, however site 02 veers to the right, not the Ekman direction. The conflicting results make it difficult to prove any evidence of Ekman veering, this may be due to the high flow velocities of the area, which is characterized by high levels of turbulent mixing which can lead to erosion of this feature. (Simpson and Sharples, 2012) The evidence and explanation of the lower flow associated within both of these boundary layers is important to tidal stream energy production as when considering the position of a tidal turbine the optimum is in the area which will provide the greatest power available. If the decision of placing the turbine were made on a depth averaged velocity, it would ignore any changes in flow over depth, which this study has proved existence of and could allow for placement in an area of lower power potential, such as that identified within the BBL.

Table 7: Flow direction within the BBL

Data collection site	Mean flow over water column direction (°)	2.5 metres from ADCP flow direction (°)	4.5 metres from ADCP flow direction (°)	Mean flow direction within BBL (°)
01	31.681	31.74	28.91	30.33
02	41.245	43.33	43.67	43.5

Table 8: Bottom boundary layer depth

Data collection site	Mean Velocity during spring tide (m/s)	90% of mean flow cut off value (m/s)	BBL Depth (metres above ADCP)
-----------------------------	---	---	--------------------------------------

01	2.454	2.209	4.5
02	2.578	2.320	4.5

The interaction between two parts of water moving in the horizontal plain at different speeds is known as shear. This is seen particularly at the two previously discussed boundary layers. Shear is important in the development of turbulence, and at points of shear, turbulence is created. (Thorpe, 2007) He also describes turbulence as an action which causes the dispersion of material particles by stirring whilst homogenizing fluid properties by diffusion. Together the processes lead to mixing. As the large turbulent motions reduce down to smaller turbulent motions, they become so small that the energy is dissipated into the water by heat. This is where the energy from the tidal flow is transferred, reducing that in the flow. Proof of turbulence in the water column is well illustrated by the evidence of Turbulent Kinetic Energy (TKE). This is investigated at the EMEC test site at Orkney, Scotland by Osalusi et al. (2009) the results of which show the greatest amount of TKE production close to the bed, during the peak velocities flood and ebb tides. This study is of particular reference because the area is alike the Big Russel. It too is characterized by high tidal velocities in a similar water depth. This is also shown by Rippeth et al. (2002) in similar conditions.

The ADCP data only resolves in the vertical plain. This proves that turbulence occurs within the BBL.

The turbulence and change in velocity over the depth can also have an effect on the considerations upon designing a turbine. As shown by this study, the velocity of a tidal flow can vary greatly with depth, if a tidal turbine was designed to work in a uniform velocity over depth and were installed in a location such as the Big Russel, the loading the device was engineered for across the rotor would be significantly different to that which occurred, leading to vibration or fatigue issues endangering the working life of the device. (Osalusi et al. 2009) (Milne et al. 2013)

8.0 Conclusions

ADCP data provided by GRET of waters surrounding the island of Guernsey in the Big Russel channel and the waters close to Sark were used to carry out tidal stream resource assessments using two industry standard methodologies by EMEC and EQUIMAR. The methods were compared in structure and result output. Physical processes occurring in the water column which effects upon results are ignored were investigated. The major findings of this research are as follows:

- The results of the two resource assessments come to the same result as they use the same basic power equation. Site 01 produces the most power available over the data collection time, site 02 the second most and site 03 the least.
- The two resource assessments share a similar core structure. There are several differences within this structure between the two methods.
- The EMEC method uses velocity for calculating the occurrence percentage time which a tidal stream is at a set value. Whereas the EQUIMAR method uses the stream power for a similar style power exceedence graph. The EQUIMAR method is deemed the best as the stream power is directly proportional to the overall power.

Another difference is the contrasting methods for determining the dominance of the tidal constituents over a tidal flow. The EMEC method uses tidal ellipses calculated from the tidal harmonic analysis and the EQUIMAR version uses M2 and S2 constituent tidal profiles, fitted against the overall tidal profile. The EMEC method is better as it is a quantifiable method, whereas the EQUIMAR method is subjective.

- The presence of physical processes effecting the tidal flow were proved by the presence of residual currents of up to 0.7 m/s, not explained by tidal constituents. The physical processes included: flow retardation in the flow closest to the surface caused by wind driven currents and wave driven currents. At the BBL flow retardation was also found due to the frictional effects of the interaction between the seabed and the current. The presence of Ekman veering was not confirmed, however alteration of the angle of the flow was observed and values found in other studies are assessed. The presence of the flows changing in velocity over depth suggests that shear would have occurred, thus resulting in turbulence. The presence of turbulence can have serious implications on the structural integrity of turbines.

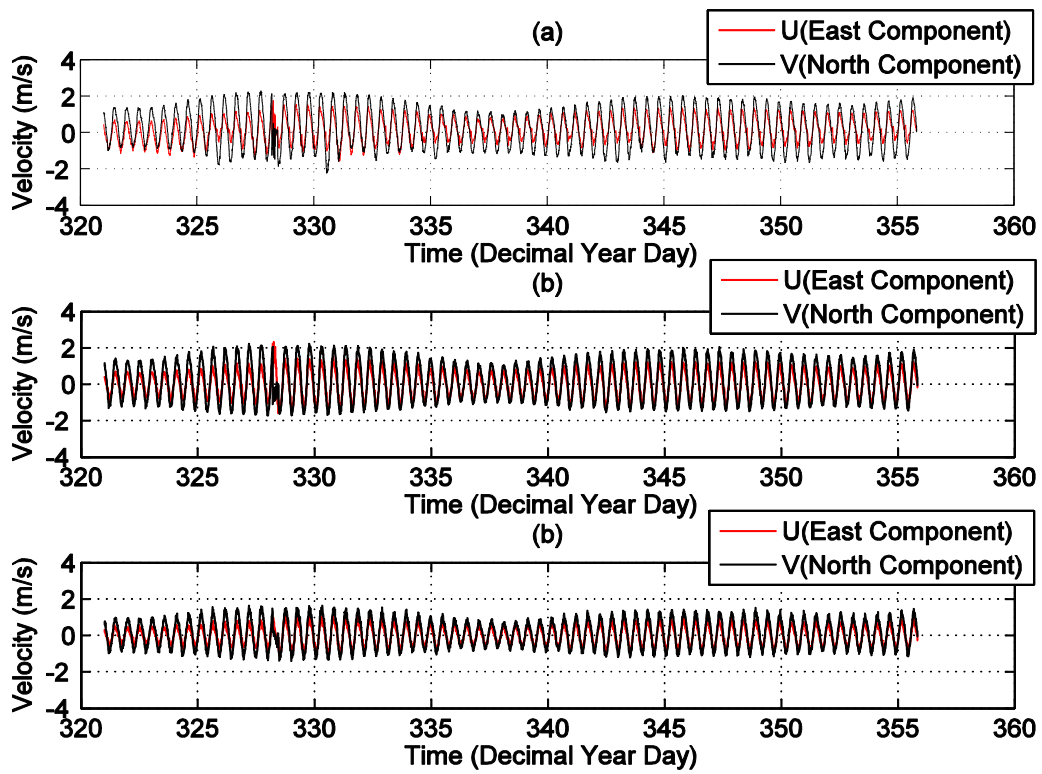
9.0 Bibliography

- Abundo, M. et al., 2012. A Combined Multi-Site and Multi-Device Decision Support System for Tidal In-Stream Energy. *Energy Procedia*, 14, pp.812–817.
- Atwater, J.F. & Lawrence, G. a, 2011. Regulatory, design and methodological impacts in determining tidal-in-stream power resource potential. *Energy Policy*, 39(3), pp.1694–1698.
- Bahaj, AbuBakr S., 2011. Generating electricity from the oceans. *Renewable and Sustainable Energy Reviews*, 15(7), pp.3399–3416.

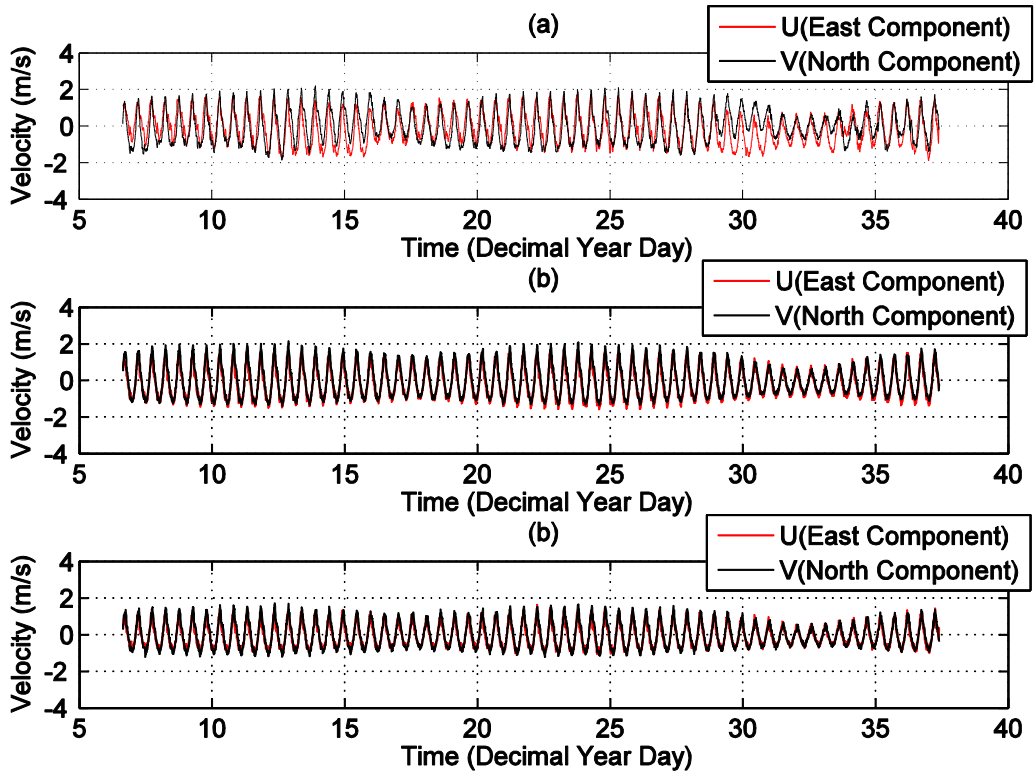
- Baños, R. et al., 2011. Optimization methods applied to renewable and sustainable energy: A review. *Renewable and Sustainable Energy Reviews*, 15(4), pp.1753–1766.
- Blunden, L.S. & Bahaj, a S., 2007. Tidal energy resource assessment for tidal stream generators. *Proceedings of the Institution of Mechanical Engineers, Part A: Journal of Power and Energy*, 221(2), pp.137–146.
- Blunden, L.S., Bahaj, a S. & Aziz, N.S., 2012. Tidal current power for Indonesia? An initial resource estimation for the Alas Strait. *Renewable Energy*, 49, pp.1–6. Available at: <http://eprints.soton.ac.uk/341106/> [Accessed February 11, 2013].
- Blunden, L.S. & Bahaj, A S, 2006. Initial evaluation of tidal stream energy resources at Portland Bill, UK. *Renewable Energy*, 31(2), pp.121–132.
- Brooks, D. a, 2006. The tidal-stream energy resource in Passamaquoddy–Cobscook Bays: A fresh look at an old story. *Renewable Energy*, 31(14), pp.2284–2295.
- Cushman-roisin, B. & Beckers, J., 2010. *Introduction to Geophysical Fluid Dynamics Physical and Numerical Aspects*.
- Ehrnström, M. & Villari, G., 2008. Linear water waves with vorticity: Rotational features and particle paths. *Journal of Differential Equations*, 244(8), pp.1888–1909.
- Legrand, C. & EMEC, 2009. *Assessment of Tidal Energy Resource*,
- Magar, V. et al., 2013. Wave Energy Resource Characterisation for Guernsey Island (UK).
- Milne, I. a. et al., 2013. Blade loads on tidal turbines in planar oscillatory flow. *Ocean Engineering*, 60, pp.163–174.
- Osalusi, E., Side, J. & Harris, R., 2009. Structure of turbulent flow in EMEC's tidal energy test site. *International Communications in Heat and Mass Transfer*, 36(5), pp.422–431.
- Pawlowicz, R., B. Beardsley, and S. Lentz, "Classical Tidal "Harmonic Analysis Including Error Estimates in MATLAB using t_tide", *Computers and Geosciences*, 28, 929-937 (2002).
- Previsic, M. et al., 2005. Survey and Characterization Tidal In Stream Energy Conversion (TISEC) Devices.
- Rippeth, T.P., Williams, E. & Simpson, J.H., 2002. Reynolds Stress and Turbulent Energy Production in a Tidal Channel. *Journal of Physical Oceanography*, 32, pp.1242–1251.
- Storlazzi, C.. et al., 2004. Wave- and tidally-driven flow and sediment flux across a fringing coral reef: Southern Molokai, Hawaii. *Continental Shelf Research*, 24(12), pp.1397–1419.
- Venugopal, V. et al., 2011. *Equitable Testing and Evaluation of Marine Energy Extraction*,

10. Appendix

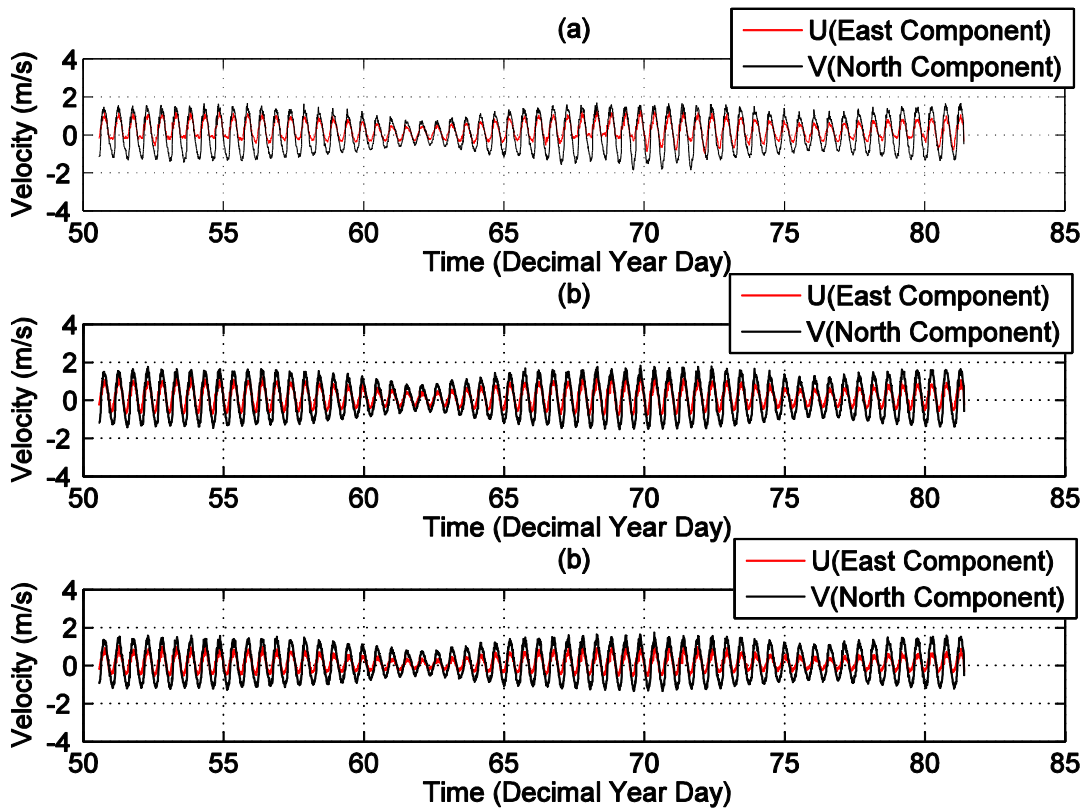
APPENDIX 1: U AND V COMPONENT TIDAL FLOW



App. 1a) U and V components of tidal flow over data collection period at site 01 over depths a)top b)mid c) bed.

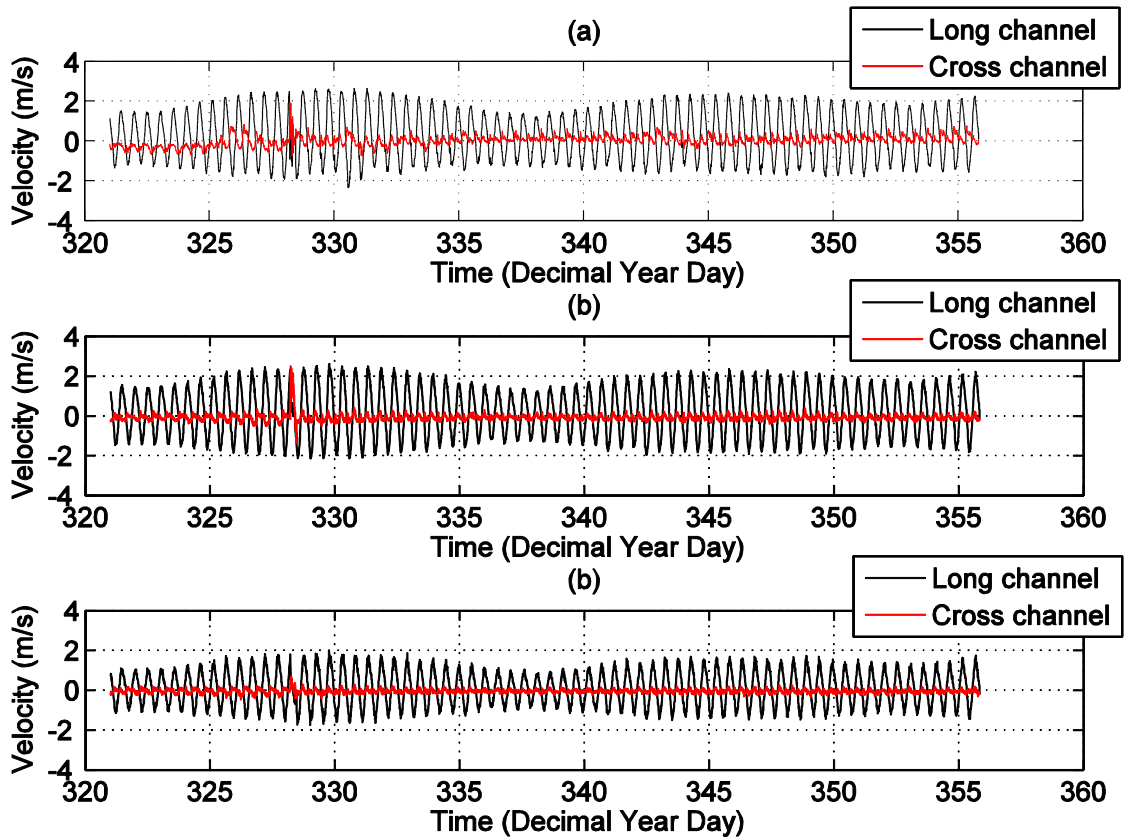


App. 1b) U and V components of tidal flow over data collection period at site 02 over depths a)top b)mid c) bed.

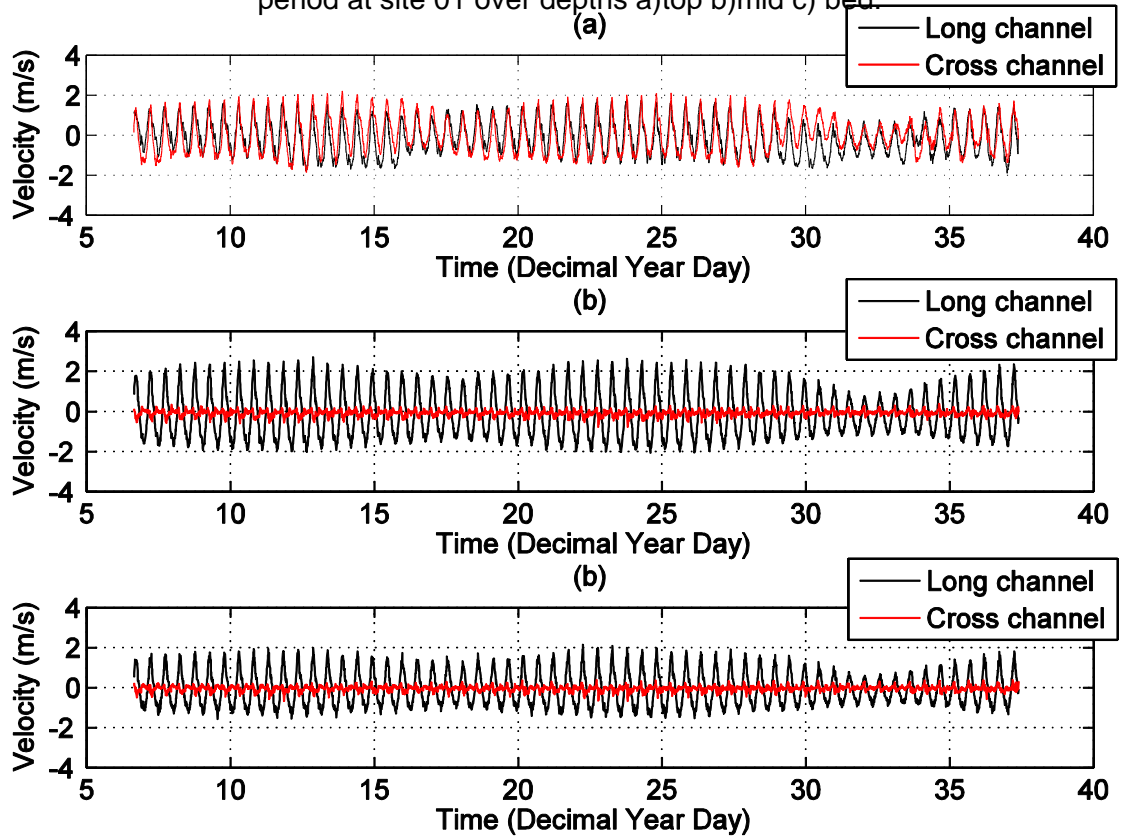


App. 1c) U and V components of tidal flow over data collection period at site 03 over depths a)top b)mid c) bed.

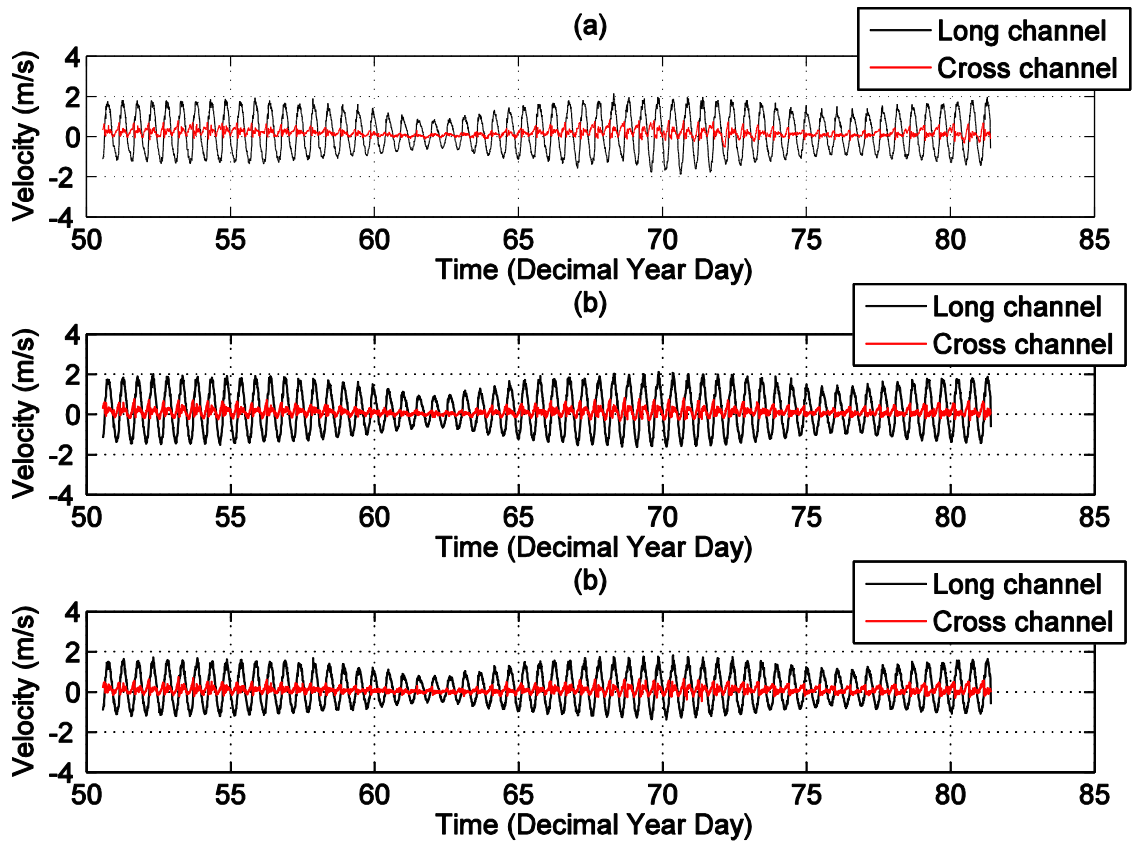
APPENDIX 2: LONG AND CROSS CHANNEL COMPONENTS OF TIDAL FLOW



App. 2a) Long and cross channel components of tidal flow over data collection period at site 01 over depths a)top b)mid c) bed.

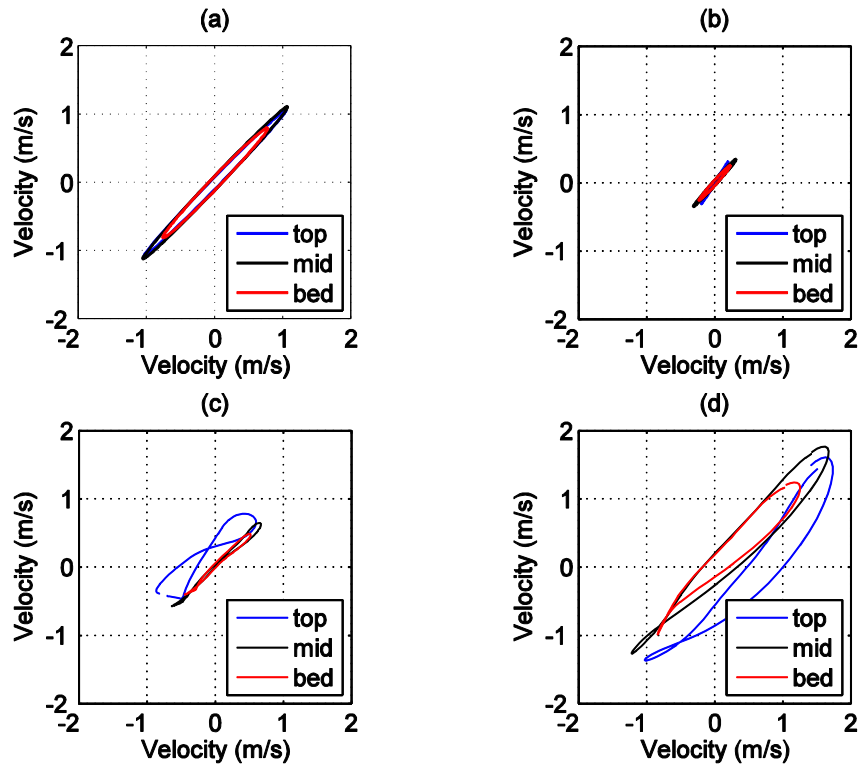


App. 2b) Long and cross channel components of tidal flow over data collection period at site 03 over depths a)top b)mid c) bed.

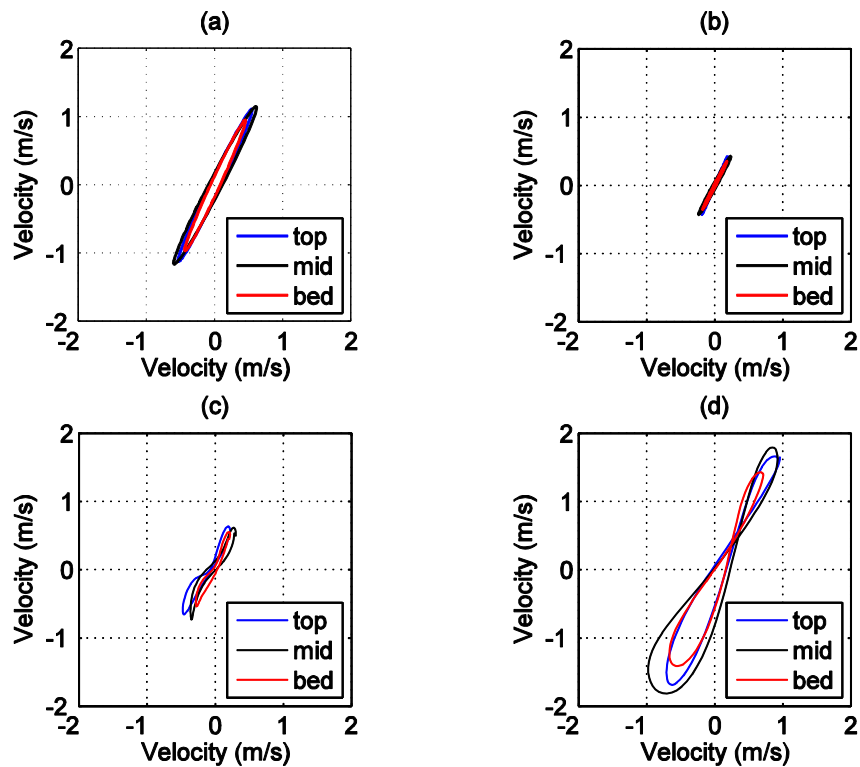


App. 2c) Long and cross channel components of tidal flow over data collection period at site 03 over depths a)top b)mid c) bed.

APPENDIX 3: TIDAL ELLIPSES AND HODOGRAPHS



App. 3a) Tidal ellipses at site 02 of a) M2 and b) S2 tidal constituents over 3 depths in water column and tidal hodographs of c) neap and d) spring tidal cycles.



App. 3b) Tidal ellipses at site 03 of a) M2 and b) S2 tidal constituents over 3 depths in water column and tidal hodographs of c) neap and d) spring tidal cycles.

APPENDIX 4: TIDAL CONSTITUENTS CALCULATED FROM TIDAL HARMONIC ANALYSIS

App. 4a) Abbreviations and full description of tidal constituents used.

Tidal constituent abbreviation	Full tidal constituent name
Mm	Lunar monthly
2Q1	Larger elliptic diurnal
Q1	Larger lunar elliptic diurnal
MSF	Lunisolar synodic fortnightly
K1	Lunar diurnal
NO1	Diurnal constituent
OO1	Lunar diurnal
O1	Lunar diurnal
N2	Larger lunar elliptic semidiurnal
M2	Principal lunar semidiurnal
L2	Smaller lunar elliptic semidiurnal
S2	Principal solar semidiurnal
ETA2	Semi Diurnal constituent
MN4	Shallow water quarter diurnal
M3	Lunar terdiurnal
M4	Shallow water overtides of principal lunar
MS4	Shallow water quarter diurnal
MK3	Shallow water terdirunal
MK5	Shallow water terdiurnal
2MN6	Shallow water sixth diurnal
M6	Shallow water overtides of principal lunar
2MS6	Shallow water quarter diurnal
M8	Shallow waer eight diurnal

App. 4b) Description of tidal harmonic analysis parameters and abbreviations used in tidal constituents.

Tidal harmonic analysis parameter abbreviation	Tidal harmonic analysis parameter	Description of parameter
Freq	Frequency	Frequency of tidal constituents (cycles/hr)
Major	Semi-major component	Constituent major axis vector (m/s)
Minor	Semi-minor component	Constituent minor axis vector (m/s)

Inc	Inclination	Ellipse orientations (degrees)
Pha	Phase	Constituent phases (degrees relative to Greenwich)
Snr	Signal to noise ratio	←

App. 4c) Tidal constituents of the tide located at site 01 at the mid depth.

Tide	Freq	Major	Minor	Inc	Pha	Snr
MSF	0.0028219	0.062	0.005	59.98	179.52	9.6
N2	0.0789992	0.306	0.034	56.54	248.24	1.1e+002
M2	0.0805114	1.685	0.062	56.39	124.82	3.2e+003
L2	0.0820236	0.129	0.022	58.01	195.79	16
S2	0.0833333	0.394	0.015	54.37	282.27	2.2e+002
ETA2	0.0850736	0.050	0.003	76.85	308.62	3.5
MN4	0.1595106	0.053	-0.013	44.43	254.60	11
M4	0.1610228	0.130	-0.028	30.90	137.48	74
MS4	0.1638447	0.055	-0.015	23.38	298.61	17
2MN6	0.2400221	0.037	0.001	64.75	30.86	4.7
M6	0.2415342	0.066	-0.004	61.21	286.37	21
2MS6	0.2443561	0.032	-0.002	60.77	70.70	4.4
M8	0.3220456	0.020	0.003	1.31	316.24	6.1

App. 4d) Tidal constituents of the tide located at site 01 at the bed depth.

Tide	Freq	Major	Minor	Inc	Pha	Snr
Mm	0.0015122	0.019	-0.004	69.89	200.12	3.4
Msf	0.0028219	0.044	0.002	58.42	179.80	19
Eps2	0.0761773	0.024	-0.008	78.91	306.44	3.3
N2	0.0789992	0.211	0.030	59.05	249.40	1.6e+002
M2	0.0805114	1.181	0.045	56.94	124.22	6.7e+003
L2	0.0820236	0.087	0.020	53.33	198.32	26
S2	0.0833333	0.279	0.002	55.91	283.83	3.2e+002
Eta2	0.0850736	0.038	0.003	67.77	320.47	6
Mn4	0.1595106	0.041	-0.015	44.25	251.20	14
M4	0.1610228	0.092	-0.033	32.71	136.99	73

Ms4	0.1638447	0.045	-0.016	30.07	293.66	25
2mn 6	0.2400221	0.018	0.000	79.86	54.16	3.4
M6	0.2415342	0.035	0.002	64.77	297.94	15
2ms6	0.2443561	0.019	-0.002	62.19	82.30	4.1
M8	0.3220456	0.013	0.002	129.75	126.99	3.5

App. 4e) Tidal constituents of the tide located at site 02 at the top depth.

Tide	Freq	Major	Minor	inc	Pha	Snr
*MSF	0.0028219	0.352	0.015	141.68	196.67	2.2
*2Q1	0.0357064	0.059	0.026	148.06	292.44	2.5
*Q1	0.0372185	0.055	0.004	129.09	170.61	2.8
*N2	0.0789992	0.193	0.007	55.51	202.58	5.1
*M2	0.0805114	1.491	0.064	45.75	144.40	4e+002
*S2	0.0833333	0.455	0.020	49.60	222.59	42
*M4	0.1610228	0.255	0.133	27.00	238.23	12
*MS4	0.1638447	0.197	0.037	63.93	325.32	6.8
*2MK5	0.2028035	0.017	0.000	71.24	266.66	2.4
*M6	0.2415342	0.070	0.036	75.27	34.30	7.1
*2MS6	0.2443561	0.085	0.020	70.30	103.57	9.8
*M8	0.3220456	0.046	0.023	36.81	154.79	4.3

App. 4f) Tidal constituents of the tide located at site 02 at the mid depth.

tide	freq	major	minor	inc	pha	snr
*O1	0.0387307	0.022	0.002	30.93	315.54	6.9
*N2	0.0789992	0.205	0.020	52.35	200.67	9.4
*M2	0.0805114	1.542	0.073	46.41	145.34	7.2e+002
*S2	0.0833333	0.470	0.028	48.08	220.62	44
*MK3	0.1222921	0.014	0.001	66.25	184.69	5.1
*M4	0.1610228	0.246	0.065	36.97	253.28	37
*MS4	0.1638447	0.170	0.034	38.56	324.33	21
*2MK5	0.2028035	0.013	0.002	47.47	286.00	3
*M6	0.2415342	0.055	0.028	56.61	24.12	8.6
*2MS6	0.2443561	0.065	0.026	57.33	95.89	9.8
*M8	0.3220456	0.041	0.021	33.71	153.90	5.6

App. 4g) Tidal constituents of the tide located at site 02 at the bed depth.

tide	freq	major	minor	inc	pha	snr
*O1	0.0387307	0.019	0.000	39.61	307.03	5.1
*K1	0.0417807	0.011	0.002	23.98	307.34	5.1
*N2	0.0789992	0.151	0.019	51.71	199.41	9.4
*M2	0.0805114	1.113	0.072	46.36	145.60	4.5e+002
*S2	0.0833333	0.344	0.026	47.90	221.85	56
*M4	0.1610228	0.181	0.030	30.14	258.00	26
*MS4	0.1638447	0.125	0.011	32.39	329.99	17
*2MK5	0.2028035	0.010	0.001	39.23	295.85	2.6
*M6	0.2415342	0.035	0.028	174.41	156.66	7.1
*2MS6	0.2443561	0.040	0.030	33.97	89.02	7.9
*M8	0.3220456	0.029	0.014	38.28	172.60	4.4

App. 4h) Tidal constituents of the tide located at site 03 at the top depth.

Tide	Freq	Major	Minor	Inc	Pha	Snr
*MSF	0.0028219	0.118	0.013	8.91	67.40	8.8
*NO1	0.0402686	0.021	0.001	134.00	338.33	4.6
*K1	0.0417807	0.018	0.005	109.72	40.85	2.1
*OO1	0.0448308	0.016	0.002	128.41	233.45	2.2
*N2	0.0789992	0.205	0.001	66.71	111.58	9.9
*M2	0.0805114	1.242	0.078	64.23	187.22	3.5e+002
*S2	0.0833333	0.472	0.007	66.40	263.23	56
*M3	0.1207671	0.013	0.007	6.09	168.88	2.9
*M4	0.1610228	0.158	0.015	94.53	281.68	6
*MS4	0.1638447	0.118	0.020	94.04	355.33	3.9
*M6	0.2415342	0.059	0.007	89.85	6.17	2.2
*2MS6	0.2443561	0.091	0.021	86.91	84.21	3.6

App. 4i) Tidal constituents of the tide located at site 03 at the mid depth.

Tide	Freq	Major	Minor	Inc	Pha	Snr
*MSF	0.0028219	0.055	0.008	22.15	74.35	3.6
*N2	0.0789992	0.198	0.006	65.84	112.35	5.7
*M2	0.0805114	1.305	0.094	62.44	186.91	2.2e+002
*S2	0.0833333	0.491	0.029	61.14	260.75	29
*M3	0.1207671	0.013	0.001	72.98	210.19	4.1
*M4	0.1610228	0.164	0.032	104.81	287.29	12
*MS4	0.1638447	0.124	0.019	111.26	0.49	7.9
*2MS6	0.2443561	0.072	0.005	110.93	80.31	4.3

App. 4j) Tidal constituents of the tide located at site 03 at the bed depth.

Tide	Freq	Major	Minor	Inc	Pha	Snr
*MSF	0.0028219	0.042	0.008	12.41	76.94	2.3
*O1	0.0387307	0.010	0.005	62.68	55.99	2.2
*N2	0.0789992	0.158	0.005	69.22	111.22	5.3
*M2	0.0805114	1.056	0.065	65.25	186.80	2.2e+002
*S2	0.0833333	0.397	0.014	63.18	260.66	35
*M4	0.1610228	0.113	0.005	111.42	289.07	10
*MS4	0.1638447	0.088	0.002	116.03	0.87	7
*2MS6	0.2443561	0.044	0.009	97.33	82.24	2.8
*M8	0.3220456	0.016	0.010	103.01	84.61	2.7

APPENDIX 5: MATLAB SCRIPTS USED IN DATA ANALYSIS

```
%Final script for Guernsey tidal resource assessment dissertation.
```

```
%The following script is for use with data site 1.
```

```
%Load the data file required, time values(t_??) and depth(z).
```

```
close all
```

```
%n is used for selecting the correct column from the speed and heading data
```

```
n1=1:20;
```

```
%First the speed is split into a separate workspace
```

```
speed01=sark01(:,(2*n1)-1);
```

```
%To compute the time into decimal.
```

```
%The start time of the data is put in below with the time at the beginning
```

```
%of the year.
```

```
start01=datetime(2011,11,18,00,04,11)-datetime(2011,1,1);
```

```
%This is the time difference for samples
```

```
int=1/24/6;
```

```

%The time of a standard data set length.
time01=start01:int:start01+int*(length(sark01(:,1))-1);

%This figure shows the current speed over time at a specific depth,
not
%required by the EMEC method
figure
plot(time01,speed01(:,20));
%speed shows little info other than the current speed
%no info about direction etc. which is why it has to be split into U &
V
title('Speed of current, Site 1 at 2.5 metres depth','FontSize',14);
ylabel('Current speed (m/s)');
xlabel('Time (Decimal Year Day)');
set(get(gca,'Xlabel'),'FontSize',14)
set(get(gca,'Ylabel'),'FontSize',14)
grid on
set(gca,'FontSize',14)
saveas(gcf,'speed of current_top','fig')
saveas(gcf,'speed of current_top','eps')
%This first graph can be used to spot any irregularities in the data,
for
%example if the ADCP was not recording correctly at any point, the bad
data
%can be found and cut out.

%This loops splits the current speed data into U(Northerly) and
V(Easterly)
%components.
for n1=1:20;
U01(:,n1)=sark01(:,(2*n1)-1).*sin(sark01(:,(2*n1)).*pi./180);
V01(:,n1)=sark01(:,(2*n1)-1).*cos(sark01(:,(2*n1)).*pi./180);
end

%Graph shows the U and V without channel adjustment
%this plot shows the east and north components at the 2.5 metres depth
%changing the 10 below will put the data into different depth bins.
figure
plot(time01,U01(:,20),'r');
hold on
plot(time01,V01(:,20),'k');
grid on
title('U (East Component) and V (North Component) at 2.5 meters height
for Site 1','FontSize',14);
ylabel('Velocity (m/s)');
xlabel('Time (Decimal Year Day)');
legend U(East Component) V(North Component)
set(gca,'FontSize',14)
set(get(gca,'Xlabel'),'FontSize',14)
set(get(gca,'Ylabel'),'FontSize',14)
saveas(gcf,'U01_V01_top','fig')
saveas(gcf,'U01_V01_top','eps')

%This next step is used to convert U and V to along channel and across
%channel velocities, the collection point sark 01 is at 30 degrees at
the
%top
long01=V01.*cos((32/180)*pi)+U01.*sin((32/180)*pi);
cross01=U01.*cos((32/180)*pi)-V01.*sin((32/180)*pi);

%U + V components of tide graphs
%01

```

```

%top
figure
subplot(3,1,1);
plot(time01,U01(:,20),'r');
hold on
plot(time01,V01(:,20),'k');
grid on
title('(a)', 'FontSize',14);
ylim([-4 4])
ylabel('Velocity (m/s)');
xlabel('Time (Decimal Year Day)');
legend U(East Component) V(North Component)
set(gca, 'FontSize',14)
set(get(gca, 'Xlabel'), 'FontSize',14)
set(get(gca, 'Ylabel'), 'FontSize',14)
%mid
subplot(3,1,2);
plot(time01,U01(:,10),'r');
hold on
plot(time01,V01(:,10),'k');
grid on
title('(b)', 'FontSize',14);
ylim([-4 4])
ylabel('Velocity (m/s)');
xlabel('Time (Decimal Year Day)');
legend U(East Component) V(North Component)
set(gca, 'FontSize',14)
set(get(gca, 'Xlabel'), 'FontSize',14)
set(get(gca, 'Ylabel'), 'FontSize',14)
%bed
subplot(3,1,3);
plot(time01,U01(:,1),'r');
hold on
plot(time01,V01(:,1),'k');
grid on
title('(b)', 'FontSize',14);
ylim([-4 4])
ylabel('Velocity (m/s)');
xlabel('Time (Decimal Year Day)');
legend U(East Component) V(North Component)
set(gca, 'FontSize',14)
set(get(gca, 'Xlabel'), 'FontSize',14)
set(get(gca, 'Ylabel'), 'FontSize',14)

%Calculation of the vertical profile at the maximum ebb flood.
%locate max flow from previous plots and marking with data point.
%Max flood and ebb flow vert prof
figure
%ebb
subplot(3,1,1);
plot(speed01(1233,:),z01,'LineWidth',2);
hold on
%flood
plot(speed01(1265,:),z01,'k','LineWidth',2);
legend Ebb Flood
xlim([1.2 3]);
ylim([0 50]);
grid on
title('(a)', 'FontSize',14);
ylabel('Depth (m)');
xlabel('Current Speed (m/s)');
set(gca, 'FontSize',14)
set(gca, 'YTick', [0 10 20 30 40 50])

```

```

set(get(gca,'Xlabel'),'FontSize',14)
set(get(gca,'Ylabel'),'FontSize',14)

%Tidal harmonic analysis
XIN01=U01+sqrt(-1)*V01;

%Define height
z01=[2.5:2:40.5];

D_top= 20; %Specify the depth cell for which you're doing the analysis
[NAME,FREQ,TIDECON,XOUT]=t_tide(XIN01(:,D_top),'interval',1/6);
%XOUT is your tidal prediction for ALL constituents!
% real(XOUT) is the U velocity component, imag(XOUT) is the V
component

%inc in the tidal output referes to the orientation of the major axis
where
%zero is east and the angle increases to the north. Therefore an angle
of
%56 degrees in inc corresponds to a heading of 90-56 = 34 degrees
north.

%Find the row corresponding to M2
m2_row01=min(find(FREQ>0.0805114));
s2_row01=min(find(FREQ>0.0833333)); %S2 constituent

%Plot tidal ellipse
coordsd1_m2top01=t_ellipse(TIDECON(m2_row01,1),TIDECON(m2_row01,3),TID
ECON(m2_row01,5));
coordsd1_s2top01=t_ellipse(TIDECON(s2_row01,1),TIDECON(s2_row01,3),TID
ECON(s2_row01,5));

%Plot predicted TOTAL TIDAL current for springs and neaps
figure
ultop01=real(XOUT);
vltop01=imag(XOUT);

%Tidal harmonic analysis
XIN01=U01+sqrt(-1)*V01;

%Define height
z01=[2.5:2:40.5];

D_mid = 10; %Specify the depth cell for which you're doing the
analysis
[NAME,FREQ,TIDECON,XOUT]=t_tide(XIN01(:,D_mid),'interval',1/6);
%XOUT is your tidal prediction for ALL constituents!
% real(XOUT) is the U velocity component, imag(XOUT) is the V
component

%inc in the tidal output referes to the orientation of the major axis
where
%zero is east and the angle increases to the north. Therefore an angle
of
%56 degrees in inc corresponds to a heading of 90-56 = 34 degrees
north.

%Find the row corresponding to M2
m2_row01=min(find(FREQ>0.0805114));
s2_row01=min(find(FREQ>0.0833333)); %S2 constituent

```

```

%Plot tidal ellipse
coordsd1_m2mid01=t_ellipse(TIDECON(m2_row01,1),TIDECON(m2_row01,3),TIDECON(m2_row01,5));
coordsd1_s2mid01=t_ellipse(TIDECON(s2_row01,1),TIDECON(s2_row01,3),TIDECON(s2_row01,5));

%Plot predicted TOTAL TIDAL current for springs and neaps
figure
ulmid01=real(XOUT);
vlmid01=imag(XOUT);

%Plot predicted TOTAL TIDAL current for springs and neaps
figure
ulmid01=real(XOUT);
vlmid01=imag(XOUT);

%Tidal harmonic analysis
XIN01=U01+sqrt(-1)*V01;

%Define height
z01=[2.5:2:40.5];

D_bed = 1; %Specify the depth cell for which you're doing the analysis
[NAME,FREQ,TIDECON,XOUT]=t_tide(XIN01(:,D_bed),'interval',1/6);
%XOUT is your tidal prediction for ALL constituents!
% real(XOUT) is the U velocity component, imag(XOUT) is the V component

%inc in the tidal output referes to the orientation of the major axis where
%zero is east and the angle increases to the north. Therefore an angle of
%56 degrees in inc corresponds to a heading of 90-56 = 34 degrees north.

%Find the row corresponding to M2
m2_row01bed=min(find(FREQ>0.0805114));
s2_row01bed=min(find(FREQ>0.0833333)); %S2 constituent

%Plot tidal ellipse
coordsd1_m2bed01=t_ellipse(TIDECON(m2_row01bed,1),TIDECON(m2_row01bed,3),TIDECON(m2_row01bed,5));
coordsd1_s2bed01=t_ellipse(TIDECON(s2_row01bed,1),TIDECON(s2_row01bed,3),TIDECON(s2_row01bed,5));

%Plot predicted TOTAL TIDAL current for springs and neaps
figure
ulbed01=real(XOUT);
vlbed01=imag(XOUT);

%tidal ellipses script
%01
%top
close all
figure
subplot(2,2,1);
m2_ellipsetop01=plot(coordsd1_m2top01(:,1),coordsd1_m2top01(:,2),'b','LineWidth',1.2);

```

```

hold on
m2_ellipsemid01=plot(coordsd1_m2mid01(:,1),coordsd1_m2mid01(:,2),'k','
LineWidth',1.2);
hold on
m2_ellipsebed01=plot(coordsd1_m2bed01(:,1),coordsd1_m2bed01(:,2),'r','
LineWidth',1.2);
legend('top','mid','bed','Location','SouthEast')
ylim([-2 2])
xlim([-2 2])
title('(a)','FontSize',14);
ylabel('Velocity (m/s)');
xlabel('Velocity (m/s)');
set(gca,'YTick',[-2 -1 0 1 2])
set(gca,'XTick',[-2 -1 0 1 2])
set(get(gca,'Xlabel'),'FontSize',14)
set(get(gca,'Ylabel'),'FontSize',14)
grid on
axis square
set(gca,'FontSize',14);

%S2 component tidal ellipse
subplot(2,2,2);
s2_ellipsetop01=plot(coordsd1_s2top01(:,1),coordsd1_s2top01(:,2),'b','
LineWidth',1.2);
hold on
s2_ellipsemid01=plot(coordsd1_s2mid01(:,1),coordsd1_s2mid01(:,2),'k','
LineWidth',1.2);
hold on
s2_ellipsebed01=plot(coordsd1_s2bed01(:,1),coordsd1_s2bed01(:,2),'r','
LineWidth',1.2);
legend('top','mid','bed','Location','SouthEast')
ylim([-2 2]);
xlim([-2 2]);
set(gca,'YTick',[-2 -1 0 1 2])
set(gca,'XTick',[-2 -1 0 1 2])
hold on
title('(b)','FontSize',14);
ylabel('Velocity (m/s)');
xlabel('Velocity (m/s)');
set(get(gca,'Xlabel'),'FontSize',14)
set(get(gca,'Ylabel'),'FontSize',14)
grid on
axis square
set(gca,'FontSize',14)

%Neap tide tidal ellipse
subplot(2,2,3);
plot(ul1top01(2388:2463),vl1top01(2388:2463),'b')
hold on
plot(ul1mid01(2388:2463),vl1mid01(2388:2463),'k')
hold on
plot(ul1bed01(2388:2463),vl1bed01(2388:2463),'r')
ylim([-2 2])
xlim([-2 2])
legend('top','mid','bed','Location','SouthEast')
set(gca,'YTick',[-2 -1 0 1 2])
set(gca,'XTick',[-2 -1 0 1 2])
title('(c)','FontSize',14);
ylabel('Velocity (m/s)');
xlabel('Velocity (m/s)');
set(get(gca,'Xlabel'),'FontSize',14)
set(get(gca,'Ylabel'),'FontSize',14)
grid on

```

```

axis square
set(gca,'FontSize',14)
hold on

%Spring tide tidal ellipse
subplot(2,2,4);
plot(ultop01(1191:1265),v1top01(1191:1265),'b')
hold on
plot(ulmid01(1191:1265),v1mid01(1191:1265),'k')
hold on
plot(ulbed01(1191:1265),v1bed01(1191:1265),'r')
ylim([-2 2])
xlim([-2 2])
legend('top','mid','bed','Location','SouthEast')
set(gca,'YTick',[-2 -1 0 1 2])
set(gca,'XTick',[-2 -1 0 1 2])
title('(d)','FontSize',14);
ylabel('Velocity (m/s)');
xlabel('Velocity (m/s)');
set(get(gca,'Xlabel'),'FontSize',14)
set(get(gca,'Ylabel'),'FontSize',14)
grid on
axis square
set(gca,'FontSize',14)

%to plot the residual currents
figure
subplot(1,3,1);
plot(time01,U01(:,10)-real(XOUT))
hold on
plot(time01,V01(:,10)-imag(XOUT),'r')
legend('U Component','V Component')
xlabel('Data point','fontsize',14)
ylabel('Velocity (m s^{-1})','fontsize',14)
set(gca,'fontsize',14)
grid on
saveas(gcf,'residual_current_top02','fig')
saveas(gcf,'residual_current_top02','eps')

%Tidal range
%To complete this section add the pressure from the original sark 01
file
%to the 41st column
%01
close all
figure
subplot(3,1,1);
Depth_av_range=mean(sark01(:,41));
Depth01_range=sark01(:,41)-Depth_av_range;
plot(time01,Depth01_range);
grid on
title('(a)','FontSize',14);
ylim([-5 5])
ylabel('Depth (m)');
xlabel('Time (Decimal Year Day- 2011)');
set(gca,'FontSize',14)
set(get(gca,'Xlabel'),'FontSize',14)
set(get(gca,'Ylabel'),'FontSize',14)

%To calculate the velocity over depth quiver plot
%make flow direction into cartesian co-ordinates
speed01=sark01(:,(2*n1)-1);
direc01=sark01(:,(2*n1));

```

```

%select data from spring tide flood
Direc_flood=direc01(1265,:);
Veloc_spring=speed01(1265,:);

mx1=[0];
my1=[0];

%To plot the mean flow direction
figure
Direc_flood_mean=mean(Direc_flood);
Veloc_spring_mean=mean(Veloc_spring);
mrdir=Direc_flood_mean*pi/180;
%change to cartesian co-ordinates
[mx,my]=pol2cart(mrdir,Veloc_spring_mean);

%to calculate the m2 tidal direction
m201dir=29.55*pi/180;
[xm201,ym201]=pol2cart(m201dir,1.62);

%Make the plot stay at 0
x1=[0,0,0,0,0,0,0,0,0,0,0,0,0,0,0,0,0,0,0,0];
y1=[0,0,0,0,0,0,0,0,0,0,0,0,0,0,0,0,0,0,0,0];

rdir = Direc_flood*pi/180;

%change to cartesian co-ordinates
[x,y] = pol2cart(rdir,Veloc_spring);

%quiver plot velocity over each depth bin
figure
quiver3(x1,y1,z01,x,y,[0,0,0,0,0,0,0,0,0,0,0,0,0,0,0,0,0,0,0,0],'k','AutoScale','off');
hold on
quiver3(mx1,my1,43,mx,my,[0],'r','AutoScale','off','LineWidth',3);
hold on
quiver3(mx1,my1,45,xm201,ym201,[0],'b','AutoScale','off','LineWidth',3);
zlabel('Distance from ADCP (m)','fontsize',14);
xlim([-2.5 2.5]);
ylim([-2.5 2.5]);
view(-162,40);
set(gca,'XTick',[-5 -2.5 0 2.5 5])
set(gca,'YTick',[-5 -2.5 0 2.5 5])
set(gca,'fontsize',14);
line([-2 -2],[-2.5 0],'color','k','LineWidth',2);
line([-2.5 -2],[-1 0],'color','k','LineWidth',2);
line([-1.5 -2],[-1 0],'color','k','LineWidth',2);
text(-2,-2,'N','fontsize',14);
line([0 0],[0 0],[2.5 45],'color','k','LineWidth',1.5);
ylabel('Velocity(m/s)','fontsize',14);
xlabel('Velocity(m/s)','fontsize',14);

%For the calculation of the histogram which shows the velocity
distribution
%curve
%1st the speed are split into bins
figure
speeds01_top=sqrt((u1top01).^2+(v1top01).^2);
a_top01=find(speeds01_top>0 & speeds01_top<0.1);
b_top01=find(speeds01_top>0.1 & speeds01_top<0.2);
c_top01=find(speeds01_top>0.2 & speeds01_top<0.3);

```

```

d_top01=find(speeds01_top>0.3 & speeds01_top<0.4);
e_top01=find(speeds01_top>0.4 & speeds01_top<0.5);
f_top01=find(speeds01_top>0.5 & speeds01_top<0.6);
g_top01=find(speeds01_top>0.6 & speeds01_top<0.7);
h_top01=find(speeds01_top>0.7 & speeds01_top<0.8);
i_top01=find(speeds01_top>0.8 & speeds01_top<0.9);
j_top01=find(speeds01_top>0.9 & speeds01_top<1.0);
k_top01=find(speeds01_top>1.0 & speeds01_top<1.1);
l_top01=find(speeds01_top>1.1 & speeds01_top<1.2);
m_top01=find(speeds01_top>1.2 & speeds01_top<1.3);
n_top01=find(speeds01_top>1.3 & speeds01_top<1.4);
o_top01=find(speeds01_top>1.4 & speeds01_top<1.5);
p_top01=find(speeds01_top>1.5 & speeds01_top<1.6);
q_top01=find(speeds01_top>1.6 & speeds01_top<1.7);
r_top01=find(speeds01_top>1.7 & speeds01_top<1.8);
s_top01=find(speeds01_top>1.8 & speeds01_top<1.9);
t_top01=find(speeds01_top>1.9 & speeds01_top<2.0);
u_top01=find(speeds01_top>2.0 & speeds01_top<2.1);
v_top01=find(speeds01_top>2.1 & speeds01_top<2.2);
w_top01=find(speeds01_top>2.2 & speeds01_top<2.3);
x_top01=find(speeds01_top>2.3 & speeds01_top<2.4);
y_top01=find(speeds01_top>2.4 & speeds01_top<2.5);
z_top011=find(speeds01_top>2.5 & speeds01_top<2.6);
z_top012=find(speeds01_top>2.6 & speeds01_top<2.7);
z_top013=find(speeds01_top>2.7 & speeds01_top<2.8);

%2nd the speed bins are defined
speed_bins=0.05:0.1:2.55;

%The amount of occurrences of each velocity are plotted into each bin.
percentage_top01=[length(a_top01)/5018*100 length(b_top01)/5018*100
length(c_top01)/5018*100 length(d_top01)/5018*100
length(e_top01)/5018*100 length(f_top01)/5018*100
length(g_top01)/5018*100 length(h_top01)/5018*100
length(i_top01)/5018*100 length(j_top01)/5018*100
length(k_top01)/5018*100 length(l_top01)/5018*100
length(m_top01)/5018*100 length(n_top01)/5018*100
length(o_top01)/5018*100 length(p_top01)/5018*100
length(q_top01)/5018*100 length(r_top01)/5018*100
length(s_top01)/5018*100 length(t_top01)/5018*100
length(u_top01)/5018*100 length(v_top01)/5018*100
length(w_top01)/5018*100 length(x_top01)/5018*100
length(y_top01)/5018*100 length(z_top011)/5018*100];
plot(speed_bins,percentage_top01,'LineWidth',2) %You'll need the same
number of percentages as the number of speed bins
ylabel('Occurrence likelihood, (% time)', 'FontSize',14)
xlabel('Velocity, (m s^{-1}) ', 'FontSize',14)
title('Velocity distribution curve', 'FontSize',14);
set(gca, 'FontSize',14)
grid on

%Power calculations section
%transform data into absolute values.
long01a=abs(long01);
%Velocity cubed
V_cubed_top01=(long01a(:,20).^3);
V_cubed_mid01=(long01a(:,10).^3);
V_cubed_bed01=(long01a(:,1).^3);
V_cubed_av01=(mean(long01a.')).^3);

%power equation for EQUIMAR, not over cross-sectional area
Power_pre01equi=(0.5*1025);

```

```

%1st half of power equation over device
Power_pre01=(0.5*1025*318);

%Power availible at each 10 min interval per metre cubed
Power_availible_top01_equi=(Power_pre01equi*V_cubed_top01)/1000;
Power_availible_mid01_equi=(Power_pre01equi*V_cubed_mid01)/1000;
Power_availible_bed01_equi=(Power_pre01equi*V_cubed_bed01)/1000;
Power_availible_av01_equi=(Power_pre01equi*V_cubed_av01)/1000;

%Average power availible per metre cubed
Power_availible_top_01_equi_av=mean(Power_availible_top01_equi);
Power_availible_mid_01_equi_av=mean(Power_availible_mid01_equi);
Power_availible_bed_01_equi_av=mean(Power_availible_bed01_equi);
Power_availible_av_01_equi_av=mean(Power_availible_av01_equi);

%Power availible at each 10 min interval over device
Power_availible_top01=Power_pre01*V_cubed_top01/1000;
Power_availible_mid01=Power_pre01*V_cubed_mid01/1000;
Power_availible_bed01=Power_pre01*V_cubed_bed01/1000;
Power_availible_av01=Power_pre01*V_cubed_av01/1000;

%Average power availible over device
Power_availible_top_01_av_device=mean(Power_availible_top01);
Power_availible_mid_01_av_device=mean(Power_availible_mid01);
Power_availible_bed_01_av_device=mean(Power_availible_bed01);
Power_availible_av_01_av_device=mean(Power_availible_av01);

%Total Power over data collection period m^3
Total_power_01_equi_top=sum(Power_availible_top01_equi);
Total_power_01_equi_mid=sum(Power_availible_mid01_equi);
Total_power_01_equi_bed=sum(Power_availible_bed01_equi);
Total_power_01_equi_av=sum(Power_availible_av01_equi);

%Total Power over data collection period over device
Total_power_01_device_top=sum(Power_availible_top01);
Total_power_01_device_mid=sum(Power_availible_mid01);
Total_power_01_device_bed=sum(Power_availible_bed01);
Total_power_01_device_av=sum(Power_availible_av01);

%Max power availible kW/m^3
Total_power_01_equi_top_max=max(Power_availible_top01_equi);
Total_power_01_equi_mid_max=max(Power_availible_mid01_equi);
Total_power_01_equi_bed_max=max(Power_availible_bed01_equi);
Total_power_01_equi_av_max=max(Power_availible_av01_equi);

%Max power availible kW over device
Total_power_01_device_top_max=max(Power_availible_top01);
Total_power_01_device_mid_max=max(Power_availible_mid01);
Total_power_01_device_bed_max=max(Power_availible_bed01);
Total_power_01_device_av_max=max(Power_availible_av01);

%The following text plots the histogram for the power exceedence graph
%First the bins are split up with velocities grouped.
figure
speeds_top_exce_01_top=V_cubed_top01;
a1_top_excee01=find(speeds_top_exce_01_top>0 &
speeds_top_exce_01_top<0);
a_top_excee01=find(speeds_top_exce_01_top>0 &
speeds_top_exce_01_top<1);

```

```

b_top_excee01=find(speeds_top_exce_01_top>1 &
speeds_top_exce_01_top<2);
c_top_excee01=find(speeds_top_exce_01_top>2 &
speeds_top_exce_01_top<3);
d_top_excee01=find(speeds_top_exce_01_top>3 &
speeds_top_exce_01_top<4);
e_top_excee01=find(speeds_top_exce_01_top>4 &
speeds_top_exce_01_top<5);
f_top_excee01=find(speeds_top_exce_01_top>5 &
speeds_top_exce_01_top<6);
g_top_excee01=find(speeds_top_exce_01_top>6 &
speeds_top_exce_01_top<7);
h_top_excee01=find(speeds_top_exce_01_top>7 &
speeds_top_exce_01_top<8);
i_top_excee01=find(speeds_top_exce_01_top>8 &
speeds_top_exce_01_top<9);
j_top_excee01=find(speeds_top_exce_01_top>9 &
speeds_top_exce_01_top<10);
k_top_excee01=find(speeds_top_exce_01_top>10 &
speeds_top_exce_01_top<11);
l_top_excee01=find(speeds_top_exce_01_top>11 &
speeds_top_exce_01_top<12);
m_top_excee01=find(speeds_top_exce_01_top>12 &
speeds_top_exce_01_top<13);
n_top_excee01=find(speeds_top_exce_01_top>13 &
speeds_top_exce_01_top<14);
o_top_excee01=find(speeds_top_exce_01_top>14 &
speeds_top_exce_01_top<15);
p_top_excee01=find(speeds_top_exce_01_top>15 &
speeds_top_exce_01_top<16);
q_top_excee01=find(speeds_top_exce_01_top>16 &
speeds_top_exce_01_top<17);
r_top_excee01=find(speeds_top_exce_01_top>17 &
speeds_top_exce_01_top<18);
s_top_excee01=find(speeds_top_exce_01_top>18 &
speeds_top_exce_01_top<19);
t_top_excee01=find(speeds_top_exce_01_top>19 &
speeds_top_exce_01_top<20);

```

```

speeds_mid_exce_01_mid=v_cubed_mid01;
a1_mid_excee01=find(speeds_mid_exce_01_mid>0 &
speeds_mid_exce_01_mid<0);
a_mid_excee01=find(speeds_mid_exce_01_mid>0 &
speeds_mid_exce_01_mid<1);
b_mid_excee01=find(speeds_mid_exce_01_mid>1 &
speeds_mid_exce_01_mid<2);
c_mid_excee01=find(speeds_mid_exce_01_mid>2 &
speeds_mid_exce_01_mid<3);
d_mid_excee01=find(speeds_mid_exce_01_mid>3 &
speeds_mid_exce_01_mid<4);
e_mid_excee01=find(speeds_mid_exce_01_mid>4 &
speeds_mid_exce_01_mid<5);
f_mid_excee01=find(speeds_mid_exce_01_mid>5 &
speeds_mid_exce_01_mid<6);
g_mid_excee01=find(speeds_mid_exce_01_mid>6 &
speeds_mid_exce_01_mid<7);
h_mid_excee01=find(speeds_mid_exce_01_mid>7 &
speeds_mid_exce_01_mid<8);
i_mid_excee01=find(speeds_mid_exce_01_mid>8 &
speeds_mid_exce_01_mid<9);
j_mid_excee01=find(speeds_mid_exce_01_mid>9 &
speeds_mid_exce_01_mid<10);

```

```

k_mid_excee01=find(speeds_mid_exce_01_mid>10 &
speeds_mid_exce_01_mid<11);
l_mid_excee01=find(speeds_mid_exce_01_mid>11 &
speeds_mid_exce_01_mid<12);
m_mid_excee01=find(speeds_mid_exce_01_mid>12 &
speeds_mid_exce_01_mid<13);
n_mid_excee01=find(speeds_mid_exce_01_mid>13 &
speeds_mid_exce_01_mid<14);
o_mid_excee01=find(speeds_mid_exce_01_mid>14 &
speeds_mid_exce_01_mid<15);
p_mid_excee01=find(speeds_mid_exce_01_mid>15 &
speeds_mid_exce_01_mid<16);
q_mid_excee01=find(speeds_mid_exce_01_mid>16 &
speeds_mid_exce_01_mid<17);
r_mid_excee01=find(speeds_mid_exce_01_mid>17 &
speeds_mid_exce_01_mid<18);
s_mid_excee01=find(speeds_mid_exce_01_mid>18 &
speeds_mid_exce_01_mid<19);
t_mid_excee01=find(speeds_mid_exce_01_mid>19 &
speeds_mid_exce_01_mid<20);

```

```

speeds_bed_exce_01_bed=V_cubed_bed01;
a1_bed_excee01=find(speeds_bed_exce_01_bed>0 &
speeds_bed_exce_01_bed<0);
a_bed_excee01=find(speeds_bed_exce_01_bed>0 &
speeds_bed_exce_01_bed<1);
b_bed_excee01=find(speeds_bed_exce_01_bed>1 &
speeds_bed_exce_01_bed<2);
c_bed_excee01=find(speeds_bed_exce_01_bed>2 &
speeds_bed_exce_01_bed<3);
d_bed_excee01=find(speeds_bed_exce_01_bed>3 &
speeds_bed_exce_01_bed<4);
e_bed_excee01=find(speeds_bed_exce_01_bed>4 &
speeds_bed_exce_01_bed<5);
f_bed_excee01=find(speeds_bed_exce_01_bed>5 &
speeds_bed_exce_01_bed<6);
g_bed_excee01=find(speeds_bed_exce_01_bed>6 &
speeds_bed_exce_01_bed<7);
h_bed_excee01=find(speeds_bed_exce_01_bed>7 &
speeds_bed_exce_01_bed<8);
i_bed_excee01=find(speeds_bed_exce_01_bed>8 &
speeds_bed_exce_01_bed<9);
j_bed_excee01=find(speeds_bed_exce_01_bed>9 &
speeds_bed_exce_01_bed<10);
k_bed_excee01=find(speeds_bed_exce_01_bed>10 &
speeds_bed_exce_01_bed<11);
l_bed_excee01=find(speeds_bed_exce_01_bed>11 &
speeds_bed_exce_01_bed<12);
m_bed_excee01=find(speeds_bed_exce_01_bed>12 &
speeds_bed_exce_01_bed<13);
n_bed_excee01=find(speeds_bed_exce_01_bed>13 &
speeds_bed_exce_01_bed<14);
o_bed_excee01=find(speeds_bed_exce_01_bed>14 &
speeds_bed_exce_01_bed<15);
p_bed_excee01=find(speeds_bed_exce_01_bed>15 &
speeds_bed_exce_01_bed<16);
q_bed_excee01=find(speeds_bed_exce_01_bed>16 &
speeds_bed_exce_01_bed<17);
r_bed_excee01=find(speeds_bed_exce_01_bed>17 &
speeds_bed_exce_01_bed<18);
s_bed_excee01=find(speeds_bed_exce_01_bed>18 &
speeds_bed_exce_01_bed<19);

```

```

t_bed_excee01=find(speeds_bed_exce_01_bed>19 &
speeds_bed_exce_01_bed<20);

%To arrange the bins for the veloc power graph the text used is:
speed_ex_bins_equi=0.00:1:20.5;

%The amount of occurrences of each velocity are plotted into each bin.
percentage_top_excee01=[length(a1_top_excee01)/5018*100
length(a_top_excee01)/5018*100 length(b_top_excee01)/5018*100
length(c_top_excee01)/5018*100 length(d_top_excee01)/5018*100
length(e_top_excee01)/5018*100 length(f_top_excee01)/5018*100
length(g_top_excee01)/5018*100 length(h_top_excee01)/5018*100
length(i_top_excee01)/5018*100 length(j_top_excee01)/5018*100
length(k_top_excee01)/5018*100 length(l_top_excee01)/5018*100
length(m_top_excee01)/5018*100 length(n_top_excee01)/5018*100
length(o_top_excee01)/5018*100 length(p_top_excee01)/5018*100
length(q_top_excee01)/5018*100 length(r_top_excee01)/5018*100
length(s_top_excee01)/5018*100 length(t_top_excee01)/5018*100];
percentage_mid_excee01=[length(a1_mid_excee01)/5018*100
length(a_mid_excee01)/5018*100 length(b_mid_excee01)/5018*100
length(c_mid_excee01)/5018*100 length(d_mid_excee01)/5018*100
length(e_mid_excee01)/5018*100 length(f_mid_excee01)/5018*100
length(g_mid_excee01)/5018*100 length(h_mid_excee01)/5018*100
length(i_mid_excee01)/5018*100 length(j_mid_excee01)/5018*100
length(k_mid_excee01)/5018*100 length(l_mid_excee01)/5018*100
length(m_mid_excee01)/5018*100 length(n_mid_excee01)/5018*100
length(o_mid_excee01)/5018*100 length(p_mid_excee01)/5018*100
length(q_mid_excee01)/5018*100 length(r_mid_excee01)/5018*100
length(s_mid_excee01)/5018*100 length(t_mid_excee01)/5018*100];
percentage_bed_excee01=[length(a1_bed_excee01)/5018*100
length(a_bed_excee01)/5018*100 length(b_bed_excee01)/5018*100
length(c_bed_excee01)/5018*100 length(d_bed_excee01)/5018*100
length(e_bed_excee01)/5018*100 length(f_bed_excee01)/5018*100
length(g_bed_excee01)/5018*100 length(h_bed_excee01)/5018*100
length(i_bed_excee01)/5018*100 length(j_bed_excee01)/5018*100
length(k_bed_excee01)/5018*100 length(l_bed_excee01)/5018*100
length(m_bed_excee01)/5018*100 length(n_bed_excee01)/5018*100
length(o_bed_excee01)/5018*100 length(p_bed_excee01)/5018*100
length(q_bed_excee01)/5018*100 length(r_bed_excee01)/5018*100
length(s_bed_excee01)/5018*100 length(t_bed_excee01)/5018*100];

%The percentages must now be calculated out of 100% by subtracting
them by 100.
%01
percentage_top_power_cumsum_01=cumsum(percentage_top_excee01);
percentage_top_power_ex_01=100-percentage_top_power_cumsum_01;
percentage_mid_power_cumsum_01=cumsum(percentage_mid_excee01);
percentage_mid_power_ex_01=100-percentage_mid_power_cumsum_01;
percentage_bed_power_cumsum_01=cumsum(percentage_bed_excee01);
percentage_bed_power_ex_01=100-percentage_bed_power_cumsum_01;

%plot the power exceedence graph
plot(speed_ex_bins_equi,percentage_top_power_ex_01,'k','LineWidth',2)
hold on
plot(speed_ex_bins_equi,percentage_mid_power_ex_01,'b','LineWidth',2)
hold on
plot(speed_ex_bins_equi,percentage_bed_power_ex_01,'r','LineWidth',2)
legend Top Mid Bed
xlabel('Stream power(m/s^3) ','FontSize',14)
ylim([0 100])
set(gca,'YTick',[0 25 50 75 100])
set(gca,'FontSize',14)
grid on

```

```

%velocity comparison graph of tidal flow against tidal constituents
%M2 and S2 constituent sin wave calculation
a_M2_top_01=1.62;
a_M2_mid_01=1.685;
a_M2_bed_01=1.181;

%calculate sin wave
M2_top_01=a_M2_top_01*sin(2*pi/(12.42/24)*time01);
M2_mid_01=a_M2_mid_01*sin(2*pi/(12.42/24)*time01);
M2_bed_01=a_M2_bed_01*sin(2*pi/(12.42/24)*time01);

%S2
a_S2_top_01=0.368;
a_S2_mid_01=0.394;
a_S2_bed_01=0.279;

%calculate sin wave
S2_top_01=a_S2_top_01*sin(2*pi/(12/24)*time01);
S2_mid_01=a_S2_mid_01*sin(2*pi/(12/24)*time01);
S2_bed_01=a_S2_bed_01*sin(2*pi/(12/24)*time01);

%assign data
figure
long01top=long01(:,20);
long01mid=long01(:,10);
long01bed=long01(:,1);

%plot the spring data of flood and ebb
plot(time01(1245:1319),(long01mid(1245:1319)));
hold on
plot(time01(1245:1319),M2_mid_01(1245:1319),'r');
hold on
plot(time01(1245:1319),S2_mid_01(1245:1319),'k');
ylim([-3 3])
xlabel('Time (Decimal Year Day- 2011)','FontSize',14)
ylabel('Velocity (m/s)','FontSize',14)
set(gca,'FontSize',14)
xlim([329.6 330.2])
set(gca,'XTick',[329.6 329.8 330 330.2])
grid on
set(gca,'YTick',[-5 -4 -3 -2 -1 0 1 2 3 4 5])
legend('Long-channel velocity','M2','S2');

%plot the neap data for flood and ebb
plot(time01(2375:2445),(long01mid(2375:2445)));
hold on
plot(time01(2375:2445),M2_mid_01(2375:2445),'r');
hold on
plot(time01(2375:2445),S2_mid_01(2375:2445),'k');
ylim([-3 3])
xlabel('Time (Decimal Year Day- 2011)','FontSize',14)
ylabel('Velocity (m/s)','FontSize',14)
set(gca,'FontSize',14)
xlim([337.45 338.])
set(gca,'XTick',[337.5 337.75 338])
grid on
set(gca,'YTick',[-5 -4 -3 -2 -1 0 1 2 3 4 5])

```